5-4-1966

An Experimental Investigation Of The Continuous Penetration Of A Blunt Body Into A Simulated Cohesionless Soil.

John Lewis Colp

AN EXPERIMENTAL INVESTIGATION OF THE CONTINUOUS PENETRATION OF A BLUNT BODY INTO A SIMULATED COHESIONLESS SOIL

By

John Lewis Colp

A Thesis

Submitted in Partial Fulfillment of the

Requirements for the Degree of

Master of Science

The University of New Mexico

1965

This thesis, directed and approved by the candidate's committee, has been accepted by the Graduate Committee of the University of New Mexico in partial fulfillment of the requirements for the degree of

MASTER OF SCIENCE

Dean

5-4-66
Date

Thesis committee

Chairman

ACKNOWLEDGMENTS

The author is grateful for the ideas, the assistance, and the criticism provided by Ronald Hultgren, Walter Taylor, and Walter Dalby of Sandia Laboratory, William Hakala of the University of New Mexico, and Dean Fred Benson of Texas Agricultural and Mechanical University.

TABLE OF CONTENTS

LIST OF TABLES

LIST OF ILLUSTRATIONS

CHAPTER I

THE PROBLEM AND PURPOSE OF INVESTIGATION

The penetration of one object into a larger mass may well have been one of the earliest interests of man.[1] History shows that early man was well aware of the occurrence of the penetration event by his use of spears and other projectiles in his search for food.[2] Interest in penetration events has been continuous through man's development. Today this interest has even outstripped man's natural environment to include the serious study of penetration into extra-terrestrial bodies such as the lunar surface.

The Problem

The penetration of many materials is currently being studied by many investigators. Some of the materials being studied include metals, other structural materials, water, rocks, soils, et cetera. The purposes of these investigations are as varied as the materials being studied, ranging from scientific curiosity to survival in warfare. None of the

---

[1] Robert J. Braidwood, Prehistoric Men (Chicago: Chicago Natural History Museum, 1961).

[2] Frank C. Hibben, The Lost Americans (New York: Thomas Y. Crowell Co., 1946).

investigations conducted have achieved a clear understanding of the exact physical phenomena involved in the penetration event. It is hoped that the experimental investigation described herein may serve as a small contribution to such an understanding for the limited area that was considered.

The present investigation is concerned with the penetration of an object into the surface of the earth. Since the materials of the earth's surface range from very hard igneous rocks to water, it is apparent that such a phenomenon is extremely complex. By the selection of one specific type of earth surface material, a granular medium having no cohesion, the phenomenon can be considerably simplified. Elimination of the stratification and combinations of granular materials that exist in nature by selecting a uniform medium can result in further simplification. Finally, by deliberate selection and arrangement of the medium used as a target, a study can be performed in two dimensions rather than the three dimensions found in nature.

The problem considered by this report is to investigate, by experiments conducted at constant velocity, some aspects of the penetration of a blunt body into a two-dimensional granular target medium having no cohesion.

Purpose of the Investigation

Statement of the Purpose

It was the purpose of this investigation to utilize laboratory experimentation: (1) to compare the mechanism of continuous penetration

at constant velocity with the soil ultimate strength theory used to predict the failure of a statically loaded footing; (2) to determine the effect on resistance to continuous penetration of penetration velocity and penetrator width; and (3) to determine if the Prandtl-Terzaghi formula for bearing capacity could be used to compute the resistance to penetration of a projectile into a granular, cohesionless material.

Organization of the Remainder of the Report

The history of the development of the Prandtl-Terzaghi bearing capacity theory presently used in soil mechanics studies is described. The assumptions that were made to develop that theory are stated. The method is shown for using the bearing capacity theory to calculate the failure of a footing loaded statically. Calculations are made using that theory for the conditions under which the experimental study was performed.

A general description of the laboratory experiments using a two-dimensional simulated soil target is given. The justification for using a simulated soil medium is given. The variables considered in the experiments are described. A description is given of the equipment and method used in measuring, under dynamic conditions, the angle of internal friction of the simulated soil medium.

The effect of different velocities of penetration upon the resistance encountered is shown and discussed. The effect of the penetrator width upon resistance encountered at a constant penetration velocity is described.

A discussion is given of the failure phenomenon as postulated by the present bearing capacity theory. This is in turn compared to the failure surface observed during the experimental investigation. The effects of penetrator widths on the failure surface and the side effects that were observed are considered.

A summary of the results achieved and some conclusions that could be drawn completes this study.

CHAPTER II

PRESENT BEARING CAPACITY THEORY

Since prehistoric times the behavior of the materials of the earth's surface when subjected to loads has been of concern to man. While the systematic study of soil behavior is comparatively recent, ancient engineers were well aware of the problems involved during the founding of huge structures. Although forced to rely upon empirical determinations of bearing capacities, they succeeded surprisingly well in accomplishing their engineering objectives. Jumikis presents a well documented review of the history of the development of soil mechanics.[1]

Development of Present Theory

The bearing capacity of a soil medium is one of the most important subjects in soil mechanics. For the past two hundred years, many engineers have devoted much time to studies of the mechanisms involved in the failure of soils under loads and have advanced many theories describing these mechanisms. Several analytical methods of calculating soil bearing capacity now in use are based on these various theories of soil failure.

---

[1] Alfreds R. Jumikis, Soil Mechanics (Princeton: D. Van Nostrand Company, 1962), pp. 10-26.

For example, the theory of plasticity is the basis of several analytical methods of calculating soil bearing capacity. One method stemming from the work of L. Prandtl is used here for comparison with the experimental work performed. In the early 1920's Prandtl became interested in the penetration of metal punches into softer, homogeneous, isotropic media.[2] Considering this process from a plastic equilibrium point of view, he produced an analytical method for studying the two-dimensional penetration of a vertical punch into a horizontal surface of an infinite half-space as shown in Figure 1. A detailed description of Prandtl's system of study is given by Jumikis.[3]

Adapting Prandtl's theory of plastic failure to the study of the bearing capacity of soils, Terzaghi presented a simplified method for computing bearing capacity.[4] His method which requires much less computational effort, is widely used in soil engineering work today.

---

[2]L. Prandtl, Uber die Harte plastischer Korper, Nachr. Kgl. Ges. Wiss. Gottingen, Math. Phys. Klasse, 1920.

[3]Jumikis, op. cit., pp. 618-624.

[4]Karl Terzaghi, Theoretical Soil Mechanics, (New York: John Wiley and Sons, Inc., 1943), pp. 118-134.

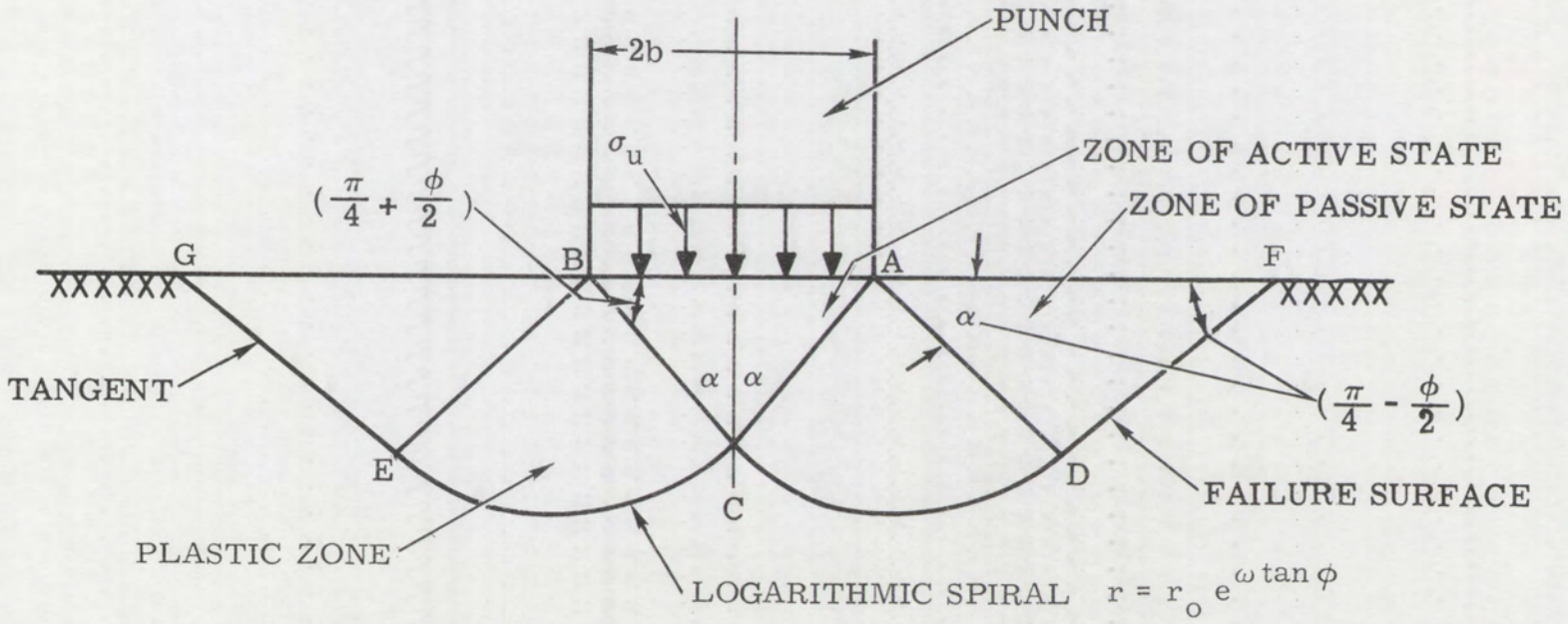

Figure 1. Prandtl's System of Study of Punch Penetration (After Jumikis[3]).

Development of the Prandtl-Terzaghi System

The Prandtl-Terzaghi system is considered as shown in Figure 2.

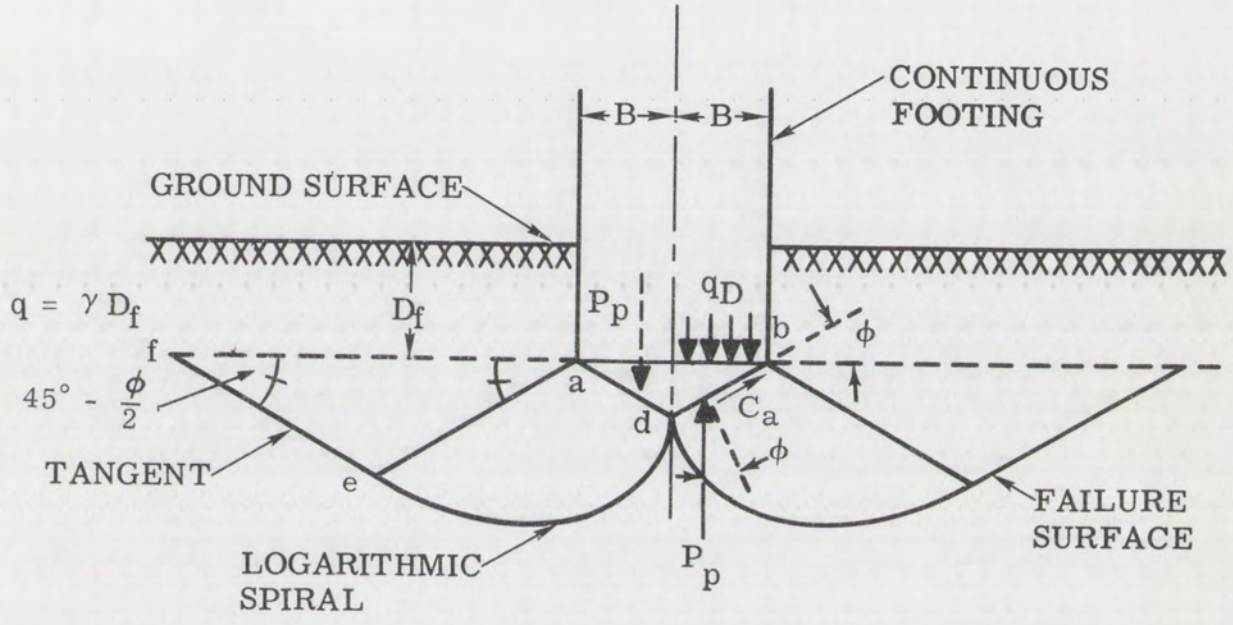

Figure 2. Prandtl-Terzaghi System of Failure Under a Footing (After Terzaghi[4])

The load at which failure occurs, Q_D, is calculated based on the principle of static equilibrium of the soil wedge zone, a b d. This principle requires that the sum of the vertical forces, including the weight of the earth in the wedge zone, should equal zero.

$$Q_D + \gamma B^2 \tan \phi - 2P_p - 2Bc \tan \phi = 0 \quad (1)$$

or

$$Q_D = 2P_p + 2Bc \tan \phi - \gamma B^2 \tan \phi \quad (2)$$

Where

Q_D = Total bearing capacity per unit of length

P_p = Passive earth pressure on one side of soil wedge a b d

2B = Footing width

c = Cohesion in Coulombs equation

ϕ = Angle of internal friction

γ = Unit weight of soil

D_f = Depth of footing below surface

q = Surcharge per unit of area

If the base of the footing rests on the horizontal surface of a half-space of cohesionless granular material for which $D_f = 0$, $q = 0$, and $c = 0$, the value for the passive earth pressure, P_p, is given by[5]

$$P_p = \frac{1}{2}\gamma H^2 \frac{K_p}{\sin\alpha \cos\delta} \tag{3}$$

Substituting in this equation $H = B \tan\phi$, $\delta = \phi$, $K_p = K_{p_\gamma}$, and $\alpha = 180 - \phi$, gives

$$P_p = \frac{1}{2}\gamma B^2 \frac{\tan\phi}{\cos^2\phi} K_{p_\gamma} \tag{4}$$

where K_{p_γ} is the coefficient of passive earth pressure for $c = 0$, $q = 0$, $\alpha = 180 - \phi$, and $\delta = \phi$. Substituting this value for P_p and the value $c = 0$ in the equation (2) for Q_D, the total bearing capacity per unit length of the footing is

$$Q_D = Q_\gamma = 2\left[\frac{1}{2}\gamma B^2 \tan\phi\left(\frac{K_{p_\gamma}}{\cos^2\varphi} - 1\right)\right] = 2B(\gamma B N_\gamma) \tag{5}$$

---

[5] Ibid, pp. 105-108.

where

$$N_\gamma = \frac{1}{2} \tan\phi \left(\frac{K_{p_\gamma}}{\cos^2 \phi} - 1 \right) \tag{6}$$

The value of K_p can be obtained by means of the spiral or the friction circle method as described by Terzaghi.[6] Since $\delta = \phi$ and $\alpha = 180 - \phi$, the values of K_{p_γ} and N_γ depend only on ϕ, the angle of internal friction of the material. The values of N_γ can be calculated.

A chart showing the relationship between N_γ and ϕ can be found in Leonards.[7]

For the case where the soil under the footing has cohesion, Terzaghi developed a simplified method for computing the ultimate bearing capacity. The expression for the normal component of the passive earth pressure, P_{p_n}, as obtained from the classical earth pressure theory, is

$$P_{p_n} = \frac{H}{\sin\alpha} \left(cK_{p_c} + qK_{p_q} \right) + \frac{1}{2} \gamma H^2 \frac{K_{p_\gamma}}{\sin\alpha} \tag{7}$$

where H is the height of the contact face, α is the slope angle of the contact face, and K_{p_c}, K_{p_q}, and K_{p_γ} are coefficients whose values are independent of H and γ. If a d in Figure 2 represents the contact face, then $H = B \tan\phi$, $\alpha = 180 - \phi$, $\delta = \phi$, $C_a = C$, and the total passive earth pressure on the contact face, P_p, is equal to $P_{pn}/\cos\delta$ or

---

[6] Ibid, pp. 108-113.

[7] G. A. Leonards, Foundation Engineering (New York: McGraw-Hill Book Co., Inc., 1962), p. 542.

$$P_p = \frac{P_{p_n}}{\cos \delta} = \frac{P_{p_n}}{\cos \phi} \tag{8}$$

Substituting the above values into equation (7) gives

$$P_p = \frac{B}{\cos^2 \phi} \left(cK_{p_c} + qK_{p_q} \right) + \frac{1}{2} \gamma B^2 \frac{\tan \phi}{\cos^2 \phi} K_{p_\gamma} \tag{9}$$

Combining equations (9) and (2) gives

$$Q_D = 2Bc \left(\frac{K_{p_c}}{\cos^2 \phi} + \tan \phi \right) + 2Bq \frac{K_{p_q}}{\cos^2 \phi}$$

$$+ \gamma B^2 \tan \phi \left(\frac{K_{p_\gamma}}{\cos^2 \phi} - 1 \right) \tag{10}$$

with K_{p_c}, K_{p_q}, and K_{p_γ} representing dimensionless coefficients independent of the width of the loaded area.

If the material in the soil wedge zone, a b d, in Figure 2 is assumed to have no weight, i.e., $\gamma = 0$, equation (10) can be written as the sum of the loads due to cohesion (Q_c) and to the surcharge (Q_q)

$$Q_c + Q_q = 2Bc \left(\frac{K_{p_c}}{\cos^2 \phi} + \tan \phi \right) + 2Bq \left(\frac{K_{p_q}}{\cos^2 \phi} \right) \tag{11}$$

$$= 2BcN_c + 2BqN_q$$

where the dimensionless coefficients N_c and N_q have values which depend only on ϕ, the angle of internal friction of the material.

Considering cohesion, c, surcharge, q, and the unit weight, γ, of the soil wedge zone, the expression for the total load at which failure occurs can be written as

$$Q_D = Q_c + Q_q + Q_\gamma = 2BcN_c + 2BqN_q + 2B^2\gamma N_\gamma \tag{12}$$

Substituting the surcharge, q, which is equal to the unit weight of the material times the depth of the bottom of the footing, γD_f, gives

$$Q_D = 2B(cN_c + \gamma D_f N_q + \gamma B N_\gamma) \tag{13}$$

Terzaghi called the coefficients N_c, N_q, and N_γ the bearing capacity factors. Their values depend only on the angle of internal friction of the material.[8] The equations for the value of N_c and N_q are derived by Terzaghi as

$$N_c = \cot\phi \left[\frac{a_\theta^2}{2\cos^2\left(45° + \frac{\phi}{2}\right)} - 1 \right] \tag{14}$$

and

$$N_q = \frac{a_\theta^2}{2\cos^2\left(45° + \frac{\phi}{2}\right)} \tag{15}$$

where

$$a_\theta = \exp\left[\left(\frac{3}{4}\pi - \frac{\phi}{2}\right)\tan\phi\right] \tag{16}$$

The values for N_γ are calculated from equation (6).

---

[8] Ibid

Assumptions of the Prandtl-Terzaghi Theory

Soils do not possess precise engineering properties. Spangler says "soils are natural materials which occur in infinite variety over the earth and whose engineering properties may vary widely from place to place within the relatively small confines of a single engineering project."[9] It is not difficult, therefore, to understand that any theory dealing with such a complicated material must make use of simplifying assumptions to achieve a manageable result. The Prandtl-Terzaghi bearing capacity theory is based on just such a series of simplifying assumptions:

1. The soil medium is homogeneous, isotropic, and an infinite half-space.
2. The footing is continuous in length.
3. The footing exerts a constant, uniform pressure on the soil medium.
4. The footing base is rough.
5. The depth of the footing below the surface is less than the footing width.
6. The soil medium fails in general shear.
7. The shearing resistance of the soil is determined by the Coulomb equation.

---

[9] M. G. Spangler, Soil Engineering, (Scranton, Pa.: International Textbook Co., 1960), p. 7.

8. Elastic deformations are small and may be ignored.
9. The soil in the wedge zone (Figure 1) behaves in an elastic manner; its deformation is ignored and it is considered to behave as a rigid body.
10. The stress in the soil wedge zone is of a hydrostatic nature.
11. The volume change in the plastic zone is zero.
12. The failure surface is a logarithmic spiral with a tangent.
13. The load on the footing is vertical and rigidly guided so that a two-sided expulsion of the soil medium occurs at failure.

CHAPTER III

THE EXPERIMENTAL INVESTIGATION

Description of the Testing Program

The objective was to perform a series of continuous vertical penetrations of a blunt body at various constant velocities into a uniform density granular target medium having no cohesion. Load resistance encountered during the penetration versus the penetration distance had to be measured. It was desirable that the mechanism of the penetration be visually observed as it progressed. It was also desirable to determine the effects of different penetrator widths upon both the load resistance and the penetration mechanism.

The equipment developed and used for this investigation* consisted of a mechanical linear actuator, a large target tank with a transparent face, an array of steel rollers, a load measuring and recording system, and a sequence camera for recording optical data. The linear actuator used was driven by a 28-volt constant speed electric motor. A pair of lead screws driven by the motor through a gear reduction system actuated a yoke. The penetrator was mounted on the yoke and was guided

---

*Development and testing of equipment to perform this investigation covered several months. Discussion of the problems involved, however, does not seem pertinent to this paper.

so that a reproducible vertical stroke was obtained. The total travel of the penetrator was about 16 inches, but the equipment was arranged so that only about 11 inches of penetration of the target medium was possible. This arrangement permitted a short no-load travel of the penetrator so that it always entered the target at a constant velocity.

The target tank was 46 inches wide by 36 inches high. It was 7/8-inch thick so that the 3/4-inch thick penetrator could enter without encountering any friction on its front or back. By making the thicknesses (z dimension) of both the target material and the penetrator the same, a true two-dimensional (x and y) test was achieved.

The front face of the target tank was 1-inch thick plexiglas to permit observation of the movement of the target material during penetration. By removing this front face, the target material could be restacked and returned to its original density, and a grid of lines could be repainted on it for the next test. Methods were developed for these operations so that they could be performed quickly and with reproducible results. The inside surface of the front face of the target tank had a grid of black lines painted over half of it.

The target material consisted of many thousands of precision-ground steel rollers of three diameters, 1/16-inch, 3/32-inch and 1/8-inch; all were 3/4-inch long and had rounded ends. The three different diameters were randomly distributed throughout the array. They were stacked in the target tank so that the length dimension coincided with the thickness of the tank.

To study movements in the target material caused by penetration forces, a 2-inch square grid of narrow white lines was painted on the front end surfaces of the stacked rollers before each test. After each test, the paint was carefully removed, the array of rollers was carefully restacked as necessary to achieve the original packing (density), and a new grid was painted for the next test.

The load measuring and recording system consisted of a linear strain gauge connected to a Brown recorder. The strain gauge assembly was calibrated before and after each test series. The Brown recorder also was calibrated immediately before and after each test. The recorder operated at a constant paper speed, and an electric clock reading in hundredths of a second was included in the pictures taken of the target tank during each test; the clock made it possible to relate load resistance to penetrator displacement independent of camera speed.

The visual observations of the operation of each test were made with a Nikon Model F single lens reflex 35 millimeter camera equipped with a battery-powered motor. All sequence photographs of the tests were taken at the fastest frame rate of the camera, between three and four frames per second. Kodak Plus X black and white film was used and full-frame 8-1/2 x 11-inch enlargements were printed with an automatic photo-printer at a constant setting to provide reproducible measurements for an entire individual test sequence. A complete set of sequence photographs from one test is included in Appendix B.

The enlarged photographs were used to obtain penetration distance versus time data which could be related to the load resistance versus time data recorded by the Brown recorder to secure the load resistance versus penetrator distance data desired. The photographs were also available for visual observations of the displacements of the target material during the penetration event.

Justification of the Simulated Soil Medium

Many investigators have performed two-dimensional tests in granular materials to observe the actions of a target material when loaded either statically or dynamically. Jumikis reports experimental studies on the shape of rupture surfaces in dry sand that have been performed since 1939.[1] These tests were run in sand boxes with one transparent side and the sand was marked into layers by the use of a dark substance. Selig and McKee report a similarly performed series of tests in which the footings were subjected to both static and dynamic loads.[2] Robinsky and Morrison performed a study of sand displacements around a model friction pile using small diameter lead shot

---

[1] A. R. Jumikis, "Rupture Surfaces in Dry Sand Under Oblique Loads," Paper No. 861, Journal of Soil Mechanics and Foundation Division, Proceedings, ASCE, Vol. 82, No. SM-1, January 1956.

[2] E. T. Selig and K. E. McKee, "Static and Dynamic Behavior of Small Footings," Journal of Soil Mechanics and Foundation Division, Proceedings, ASCE, Vol. 87, No. SM-6, December 1961, pp. 29-47.

placed in the sand. They recorded the shot movement by the use of Cobalt 60 radiographic techniques.[3]

The general program of which the work reported in this paper is a part has also included a series of two-dimensional penetrations into dry Ottawa sand. The experience gained from that series of tests indicated that a better method of studying individual particle movements in a target medium was needed. The present usage of steel rollers was one result.

The larger diameter of the steel rollers does possibly sacrifice some of the intimate interactions that might occur in a sand having a smaller particle size. However, this possible sacrifice is far overshadowed by the benefits gained from their use, namely: (1) the opportunity to clearly see and follow the exact movements of the individual particles, and (2) the performance of a true two-dimensional test in which there are no stress interactions in the thickness or "z" direction of the sample.

Variables Considered

This experimental investigation considered the following variables:

Velocity -- The average velocity of the penetrator was varied from 4.35 inches per second to 1.83 inches per second.

---

[3] E. I. Robinsky and C. F. Morrison, "Sand Displacement and Compaction Around Model Friction Piles," Canadian Geotechnical Journal, Vol. No. 1, No. 2, March 1964, pp. 81-93.

Penetrator Width -- The width (x dimension) of the parameter was varied from 1 to 3 inches.

Penetration Depth -- The depth (y dimension) of penetration was varied from 0 to 10.7 inches.

All tests were performed into a granular, inelastic material having no cohesion, a known angle of internal friction,[4] and a known density. All other conditions were held as constant as experimentally possible.

[4]The method used to measure the angle of internal friction under a dynamic load is described in Appendix A.

CHAPTER IV

EXPERIMENTAL AND ANALYTICAL RESULTS

Results of the experimental and analytical investigations conducted are reported in this chapter. The experimental data gathered are shown in tabular and graphic forms. The analysis of the experimental results is shown in graphic form. The calculations of bearing capacity using the Prandtl-Terzaghi formula are shown. The results of these calculations are tabulated. A comparison of the experimental results and calculated results is made and presented graphically. A discussion of the comparison is given.

Bearing Capacity Calculations

The Prandtl-Terzaghi bearing capacity formula described in Chapter II and shown by equation (13) was developed for the case where general shearing occurs. General shear is considered to be the situation that results when a dense, stiff, granular soil is loaded. As the load is increased, the settlements gradually increase until a loading situation is reached at which general shear failure occurs and the settlement proceeds at a much more rapid rate. Local shear is a situation that occurs when the settlements begin at a rapid rate as soon as loading is started and continue to increase as the load is increased.

Of course, in both cases, Terzaghi was considering static, not dynamic, loading conditions.

In considering the application of the Prandtl-Terzaghi formula to the dynamic penetration problem under study, it was felt that the case of general shear was applicable. This would seem logical since the target medium used was hard, dense, and granular.

The values of bearing capacity for the various test conditions considered in the experimental investigation and using the target medium properties observed were calculated as follows:

$$Q_D = 2B(cN_c + \gamma D_f N_q + \gamma B N_\gamma) \qquad (13)$$

where

B = one-half the width of the penetrator

c = 0

γ = 0.228 pounds/cubic inch (measured value)

D_f = penetration distance

ϕ = 30° (measured value, see Appendix A)

N_q = 25[1]

N_γ = 21[1]

If

$B = \frac{1}{2}$ inch (1 inch wide penetrator)

D_f = 1 inch

$Q_D = 1[(0.228)(1)(25) + (0.228)(0.5)(21)]$

$= 5.7 + 2.4 = 8.1$ pounds.

---

[1]G. A. Leonards, Foundation Engineering, (New York: McGraw-Hill Book Co., Inc., 1962), p. 542.

If

$$B = \frac{1}{2} \text{ inch}$$

$$D_f = 10 \text{ inches}$$

$$Q_D = 1[(0.228)(10)(25) + (0.228)(0.5)(21)]$$

$$= 57.0 + 2.4 = 59.4 \text{ pounds.}$$

Calculations of bearing capacity using equation (13) were made for all values of penetrator width. The results of these calculations are shown in Table I. The total load values have been converted to unit bearing pressures in pounds per square inch and tabulated also.

Experimental Results

The experimental investigations of this study were performed for two purposes; (1) to study the effect of penetrator velocity variations, and (2) to study the effect of penetrator width (x dimension) variations.

Effect of Penetrator Velocity

The series of tests performed to investigate the effects of penetrator velocity upon the penetration load versus depth relationship were all run using a 1-inch wide (x dimension) penetrator. The penetrator velocities investigated were 1.83, 2.04, 2.38, and 4.35 inches per second. All penetrator velocities are the average values recorded for the entire penetration depth.

$$Q_D = 2B(cN_c + \gamma D_f N_q + \gamma B N_\gamma)$$

where $c = 0$, $\gamma = 0.228\ \text{lb/in}^3$, $\phi = 30°$, $N_q = 25$, $N_\gamma = 21$

$$\text{Penetrator Load } (L_p) = Q_D\ (0.75)$$

$$\text{Unit Penetrator Load } (q_p) = \frac{Q_D}{2B}$$

Penetrator Width 2B (in.)	Penetrator Depth D_f (in.)	Q_D (LB/Lin. in.)	Penetrator Load L_p (LB)	Unit Penetrator Load q_p (psi)
1	1	8.1	6.1	8.1
	10	59.4	44.5	59.4
2	1	21.0	15.8	10.5
	10	123.6	92.7	61.8
3	1	38.7	29.0	12.9
	10	193.0	145.0	64.2

TABLE I

Calculated Bearing Capacity Values Prandtl-Terzaghi Formula
General Shear Case

All experimental data recorded for this test series are tabulated in Table II. The values given are for penetration depth in inches, total load on the penetrator in pounds, and unit load on the penetrator in pounds, and unit load on the penetrator in pounds per square inch.

The values of depth versus unit load for the four tests using the 1-inch wide penetrator are shown graphically on Figure 3. The values for the unit bearing pressures calculated using the Prandtl-Terzaghi general shear case formula from Table I are also plotted on Figure 3. The values for depth versus total penetrator load for the four tests and the same values calculated from the bearing capacity formula are shown graphically on Figure 4.

Increasing the velocity of penetration results in a decrease in both unit and total penetrator load as shown on Figures 3 and 4. In attempting to understand this seemingly anomalous behavior, several things have been considered.

Since this is a dynamic event in a non-continuous medium, there may be inertial effects at work whose actions are imperfectly understood. There appear to be indications that the target material behaves as a locking medium rather than in an elasto-plastic manner. Observations made during the dynamic simple shear tests described in Appendix A seemed to indicate this locking-unlocking characteristic did exist in this material.

It is conceivable that this behavior could be associated with the different values for static and kinetic friction. It may be that once the inertia effects of movement of the particles in this medium are overcome,

Test No. 16 Penetrator Velocity = 1.83 in/sec			Test No. 16A Penetrator Velocity = 2.04 in/sec			Test No. 17 Penetrator Velocity = 2.38 in/sec			Test No. 14 Penetrator Velocity = 4.35 in/sec		
Total Depth (in)	Total Load (lb)	Unit Load (psi)	Total Disp. (in)	Total Load (lb)	Unit Load (psi)	Total Disp. (in)	Total Load (lb)	Unit Load (psi)	Total Disp. (in)	Total Load (lb)	Unit Load (psi)
0	0	0	0	0	0	0	0	0	0	0	0
0.6	2	2.67	0.3	-	-	0.4	-	-	1.8	2	2.7
1.4	3	4.00	1.1	1	1.3	1.3	2	2.7	3.4	5	6.7
2.0	5	6.67	1.9	4	5.3	2.3	3	4.0	5.2	8	10.7
3.5	14	18.7	2.7	8	10.7	3.2	5	6.7	6.8	12.5	16.7
4.1	19	25.4	3.5	12	16.0	4.1	6	8.0	8.5	16	21.4
4.9	23	30.7	4.3	16	21.7	5.1	10	13.3	10.1	22	29.4
5.5	28	37.4	5.1	22	29.4	6.0	14	18.7	10.7	24	32.0
6.2	31	41.4	5.9	28	37.4	7.0	16	21.3			
7.0	32	42.7	6.7	32	42.7	7.9	19	25.3			
7.6	36	48.0	7.4	32	42.7	8.7	21	28.0			
8.4	40	53.4	8.1	38	50.7	9.6	25	33.3			
9.0	48	64.0	8.9	46	61.5	10.5	30	40.0			
9.8	57	76.0	9.6	44	59.0						
10.4	63	84.0	10.3	45	60.2						
10.6	67	89.4	10.6	46	61.5						

TABLE II

Experimental Values of Load Versus Depth for One Inch Wide Penetrator at Various Velocities of Penetration

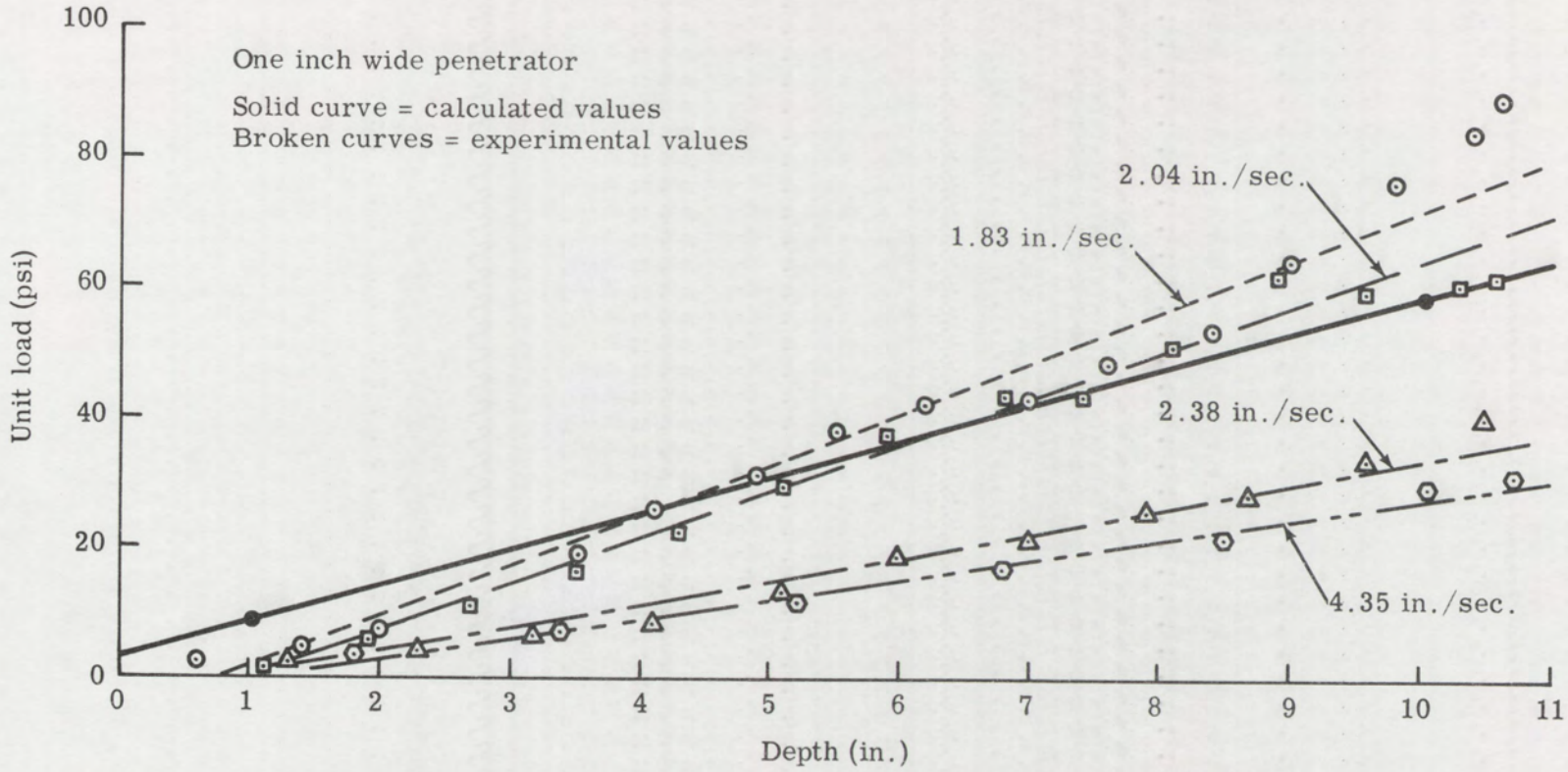

Figure 3. Unit Load vs. Depth Curves at Various Velocities of Penetration

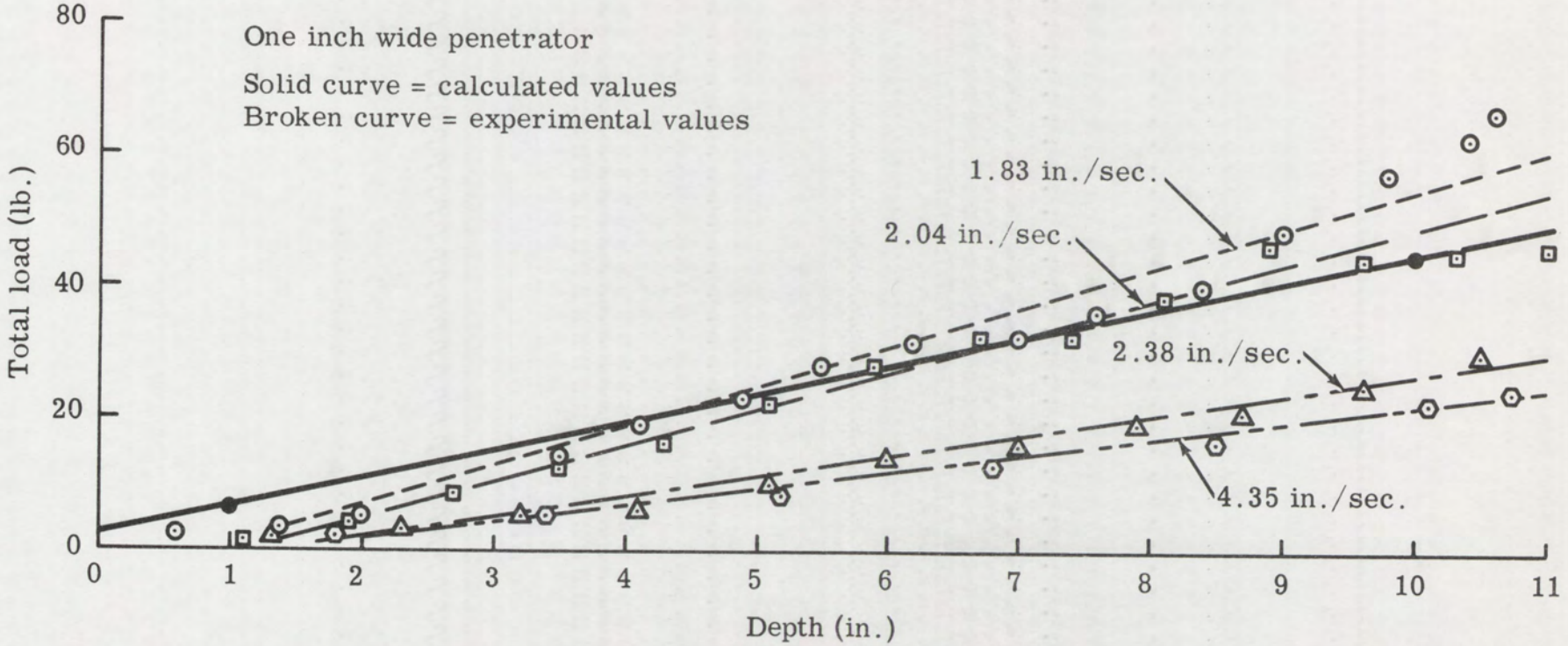

Figure 4. Total Load vs. Depth Curves at Various Velocities of Penetration

the force required to keep them in motion decreases. This, of course, is contrary to what is believed in soil mechanics to result from an increase in surcharge with increasing depth. However, it must be pointed out that little is known about soil mechanics under dynamic loading conditions.

There seems to be a slight tendency in some of the data shown for the slope of the load-depth curve to increase with increasing depth. This could indicate that the region of penetration depth investigated in this study was inadequate to secure a true insight into the actual mechanism of penetration. Also, the narrow range of penetration velocities investigated may tend to give a provincial appearance to the true actions in progress.

Vesić, Banks, and Woodard report on a series of model footing (circular, rigid, rough plates with a diameter of 4 inches) tests on dense, dry sand performed at the Georgia Institute of Technology.[2] Their Figure 7 shows a decided decrease in bearing capacity (load required for penetration) as the loading velocity was increased. The range of loading velocities at which this decrease was observed was approximately the same as the range used in the tests reported herein.

Considering the plot of the calculated values for the bearing capacity using the Prandtl-Terzaghi formula for the general shear case, the

---

[2] A. S. Vesic , D. C. Banks, and J. M. Woodard, "An Experimental Study of Dynamic Bearing Capacity of Footings on Sand," Sixth International Conference on Soil Mechanics and Foundation Engineering, Montreal, Canada, September 1965.

the experimental curves secured at penetration velocities of 1.83 and 2.04 inches per second agree rather well.

Effect of Penetrator Width

The series of tests performed to investigate the effects of penetrator width (x dimension) upon the penetration load versus depth relationship were run with penetrator widths of 1, 2, and 3 inches and a constant penetration velocity. All experimental data recorded for this test series are tabulated in Table III. The values given are for penetration depth in inches, total load on the penetrator in pounds, and unit load on the penetrator in pounds per square inch.

The values of depth versus unit load for the three tests is plotted on Figure 5. The values for the calculated unit bearing pressures from Table I are also included in Figure 5.

Figure 6 displays the depth versus total penetrator load for the experimental and calculated values.

The effect of increasing penetrator width in the experimental investigation conducted was an increase in the total force required for penetration (Figure 6). Certainly this is to be expected, but the rate of increase of force required for the experimental investigations is far smaller than that indicated by the calculated values.

Considering Figure 5, the same information has been shown except that it has been reduced to unit loads on the penetrator. This presents quite a different picture with some seemingly anomalous behavior of the experimental data immediately obvious. As shown, the unit penetrator force required for penetration decreases with increasing

Test No. 16A Penetrator Width = 1 Inch			Test No. 19 Penetrator Width = 2 Inches			Test No. 20 Penetrator Width = 3 Inches		
Depth (in)	Total Load (lb)	Unit Load (psi)	Depth	Total Load	Unit Load	Depth	Total Load	Unit Load
0	0	0	0	0	0	0	0	0
0.3	-	-	0.2	2	1.34	0.5	7	3.1
1.1	1	1.3	1.3	6	4.0	1.75	15	6.7
1.9	4	5.3	2.5	10	6.7	3.0	22	9.8
2.7	8	10.7	3.6	17	11.4	4.25	29	12.9
3.5	12	16.0	4.7	26	17.4	5.5	36	16.0
4.3	16	21.7	5.8	35	23.4	6.6	48	21.4
5.1	22	29.4	6.8	41	27.4	7.75	56	25.0
5.9	28	37.4	7.8	50	33.4	8.9	65	29.0
6.7	32	42.7	8.8	58	38.7	10.0	81	36.0
7.4	32	42.7	9.8	58	38.7	10.7	94	42.0
8.1	38	50.7	10.6	65	43.4			
8.9	46	61.5						
9.6	44	59.0						
10.3	45	60.2						
10.6	46	61.5						

TABLE III

Experimental Values of Load versus Depth for Various Penetrator Widths

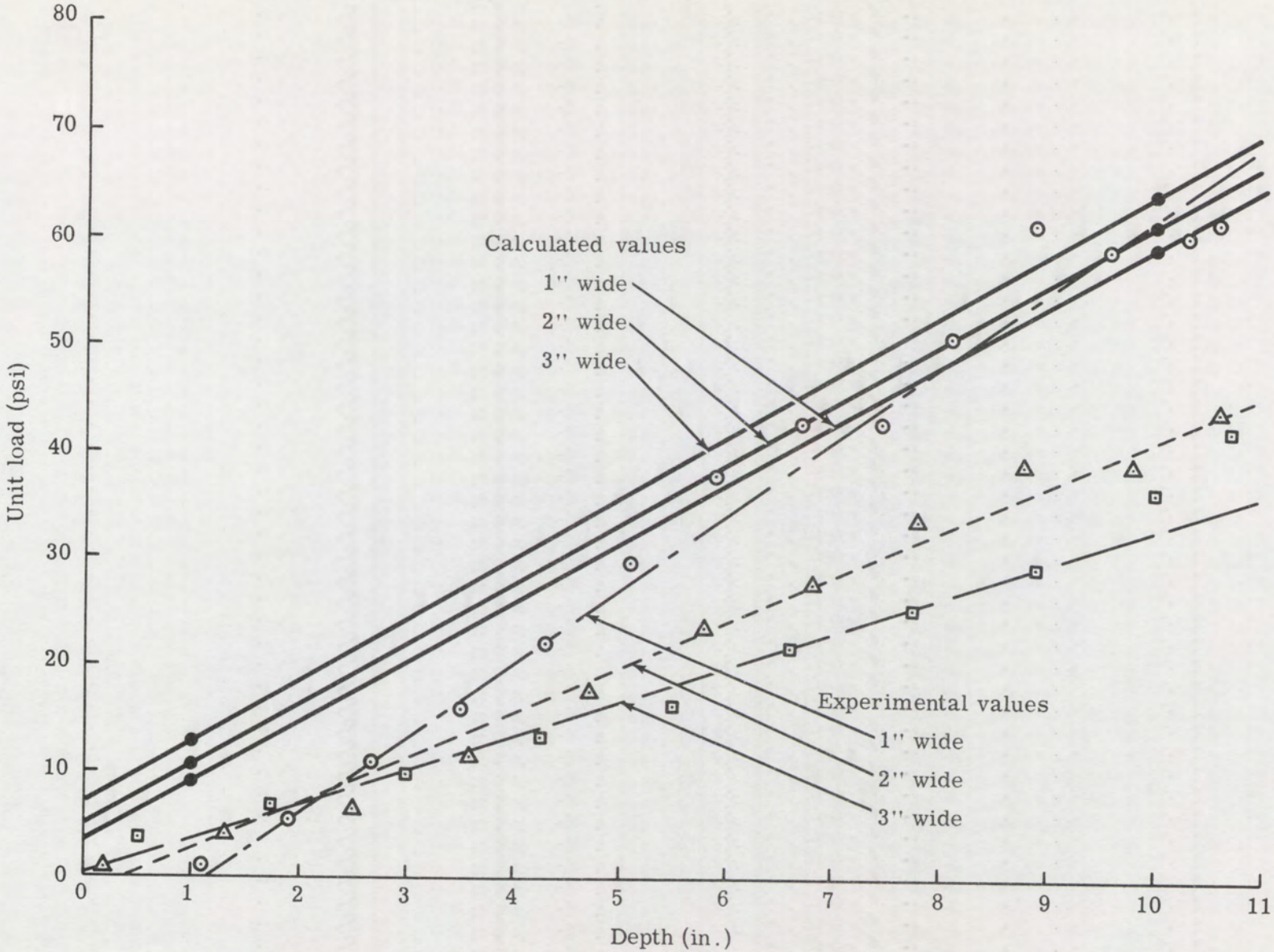

Figure 5. Unit Load vs. Depth Curves for Various Penetrator Widths

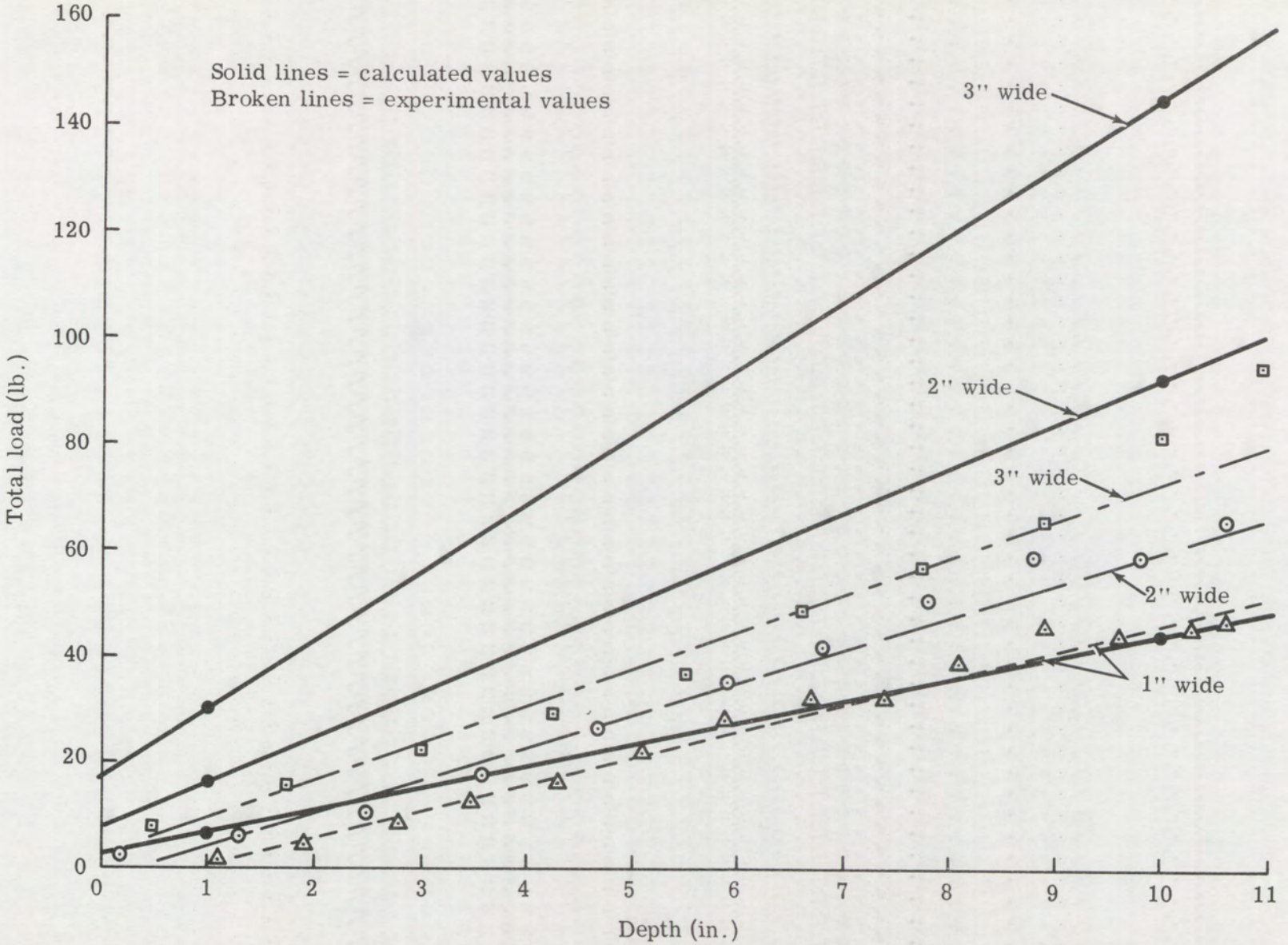

Figure 6. Total Load vs. Depth Curves for Various Penetrator Widths

penetrator width. From an intuitive standpoint, this situation does not seem reasonable. The question is immediately raised concerning possible reasons for reduction in unit force at failure with increasing penetrator width.

Such behavior might appear if the conversion of total load values to unit load values overemphasized some influence of penetrator width. Close study of particle movements during the penetration event (from the 35 mm. sequence photographs of these particular tests) indicated that the width of the slip front (Figure 7) remained essentially constant, regardless of the penetrator width. It also appeared that the area of the severe shear zone remained quite constant regardless of penetrator width. Too, the length of the shear front appeared to remain reasonably constant over the range of tests performed with different penetrator widths. These observations could contribute to an explanation of the close relationships shown by the total load values required for penetration in Figure 6. From these considerations, it would appear that under the conditions (target material, depth variations, and penetrator width variations) investigated in this study, the effect of penetrator width was not a very significant factor.

Hvorslev discusses a series of plate bearing tests that have been performed at the Waterways Experiment Station, Vicksburg, Mississippi.[3] Tests were run using three sizes of circular plates (1.4, 2.8 and 4.2 inches in diameter) which were forced into soil at a constant velocity of

---

[3] M. J. Hvorslev, Discussion at Session II - Shallow Foundations, Symposium on Bearing Capacity and Settlement of Foundations, Duke University, April 1965.

6 inches per minute. The results of plate tests into dry, uniformly graded Yuma sand in the loose and dense states are shown in his Figures 2 and 3. In each case, at a depth of about 2 inches, the unit load (in psi) decreases with increasing plate diameter. This is almost identically the behavior observed and shown in Figure 5 of this paper.

Kerisel reports on a series of pile tests performed at the Chevreuse Station near Paris, France.[4] His Figure 2 , "Point Resistance in Sand versus Depth," shows a decrease in point resistance as the pile diameter increases for a series of full-scale pile tests into a very large container (6.4 m in diameter by 10 m deep) of rounded, dry Loire river sand in a dense state. This observation agrees with that reported by Hvorslev under considerably different test conditions; and both agree with the observations reported in this paper under yet different test conditions[5]

---

[4]J. Kerisel, "Deep Foundations Basic Experimental Facts," Deep Foundations Conference, Mexico D. F., Mexico, December 1964.

[5]Hvorslev, Loc. Cit.

CHAPTER V

DESCRIPTION OF FAILURE PHENOMENON

From the observations and analysis of the results of the experimental investigation, it is clearly apparent that a complex mechanism is in operation during the failure phenomenon of a dynamic penetration event. Many investigators have studied penetration, but few have actually observed the failure mechanism in operation and none have stated a clear understanding of all that is involved. Some considerations of possible failure mechanisms as observed in this study will be made in this chapter.

Failure Phenomenon Assumed in Bearing Capacity Theory

Bearing capacity theories assume that there is one surface along which shearing proceeds when failure occurs. The failure surface due to a bearing capacity failure has been assumed to have as many shapes as there have been investigations. The shape assumed by the Prandtl-Terzaghi theory has been shown in Figure 2. A wedge of material has been assumed to form immediately under the penetrator and remain so throughout the loading cycle. The failure surface has been assumed to take a logarithmic spiral shape with straight line tangents.

Failure surfaces that have been assumed by other investigators include broken planes, circular, circular with tangents, cycloidal and spirals.

Failure Phenomenon Observed in Experimental Investigation

An examination of the photographs of the penetration events performed in this study indicates that there may well be more than one failure surface formed and more than one mode of failure operational during a dynamic penetration event. Figure 7 shows a possible interpretation of the complex phenomenon that might be occurring.

Edge Effects Zone

As can be seen, there is a region called the edge effects zone in which the target material is being dragged down with the penetrator. With the exception of the material directly under the penetrator, this edge effects zone appears to contain the only particles of the target material that are given a downward movement. The width of this edge effects zone seems to bear a direct relationship to the width of the penetrator; it affects an area about 0.6 times the penetrator width on either side of the penetrator.

Wedge Zone

Several 16 mm. high speed motion pictures taken of penetrations into the steel roller material at the same penetration velocities considered in this study show wedge of material ahead of the penetrator at all

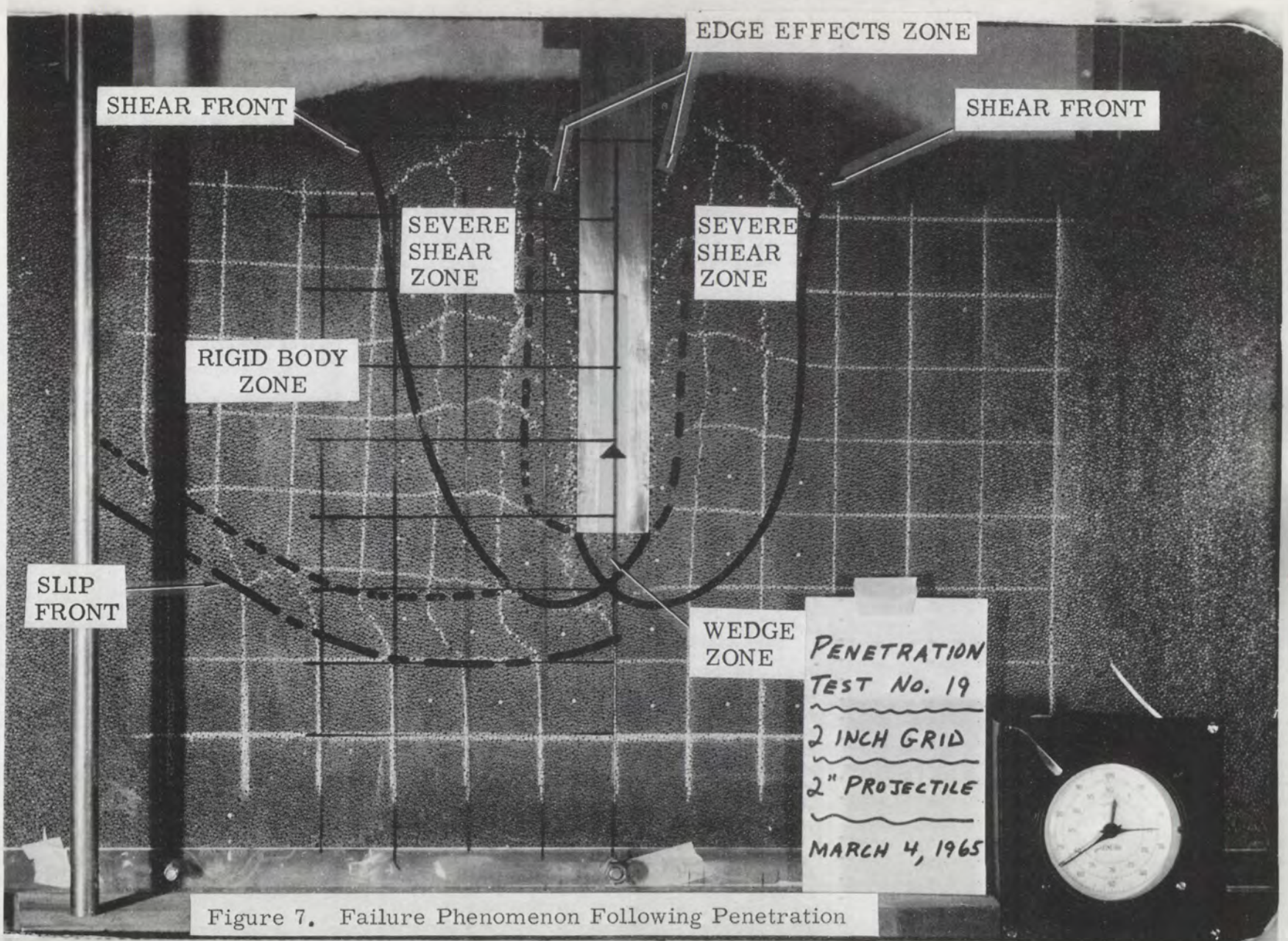

Figure 7. Failure Phenomenon Following Penetration

times during the event. This wedge is as the Prandtl-Terzaghi theory postulates. However, the motion pictures show that the particles composing this material are constantly changing during the progress of the penetrator; the wedge is there, but it is always composed of different particles. Evidence supporting this observation can be seen from the row of white bearings strung out along the left side of the penetrator in Figure 7. These white particles were originally located in the grid line directly under the centerline of the penetrator. They have passed through this constantly changing wedge of material and have been deposited along the way as the penetration progressed.

Shear Front

As dynamic penetration proceeds with depth, a zone of shearing action can be observed to be operational at all stages of penetration from surface impact until final rest. The location of the series of positions at which shearing forces between the individual particles of the target medium are operational has been defined as the shear front. This shear front resembles the familiar shock wave generated by impact loading. However, the shear front is not a wave; it is a distinct locus of points at which simple shear is occurring at a given time. Any waves generated by the penetration event have long since passed before the shear front is formed.

As penetration proceeds, the shear front is continuously moving and expanding. The particles that have been passed by the moving shear front continue to suffer shear deformation from the effects of deeper

particles through which the shear front is passing. It must be remembered that the situation shown in Figure 7 is the static result of a dynamic event. For a full understanding of what is shown there, the progress of the event to the static situation shown must be visualized. Appendix B contains a full set of sequence photographs of the penetration test which produced Figure 7. Detailed examination of the sequence photographs will aid in understanding the failure description given in this chapter.

Slip Front

A slip front, located a relatively great distance below and beyond the shear front location, was observed to form in the penetration tests performed. This slip front can be seen in Figure 7 between 12 and 14 inches below the original top surface of the target material.* The formation of this slip front can be seen in the sequence photographs in Appendix B. Initial movement can be seen on photograph 8 and complete formation is visible in photograph 9.

Consideration has been given to the forces that cause slip front formation and continuation. Slip fronts have been observed on many of the penetration tests performed; such a front appears to be a basic part of the penetration phenomenon. Since one apparent explanation is that there was a plane of weakness, density variation, or similar major discontinuity in the target medium at that location, great care was taken in the preparation of the target medium prior to a test to eliminate any lack of homogeneity.

*Each black grid square in Figure 7 is 2 inches on a side.

Measurements of the width of the slip front were made from the experimental investigation photographs. It was found to be quite consistent in width, with little variation as a result of different penetrator widths.

Severe Shear Zone

The material contained between the shear front and the penetrator has been called the severe shear zone. In this zone, all of the particles have been in a state of continuous shear during the penetration event. They were first sheared when the shear front passed them and continued to be reworked and relocated (sheared) during the remainder of the dynamic event. It is believed that the effects of inertial forces on the penetration event become significant in this region. Once the particles in this zone become mobile as a result of the passage of the shear front, perhaps some not-yet-understood mechanism becomes important.

Observation of the movements of individual particles in the severe shear zone have been made from high speed motion pictures taken of many penetration tests into the steel roller target medium. Excluding those particles located in the edge effects zone and the wedge zone where the downward motion of the penetrator is dominant, all particles inside the severe shear zone are observed to have been displaced upward and outward away from the penetrator. No downward movement is observed.

Appreciable dialation (decrease in density) of the target material can be observed in this zone. This would normally be expected as the result of shearing action in a dense, granular medium. Density change

measurements (not made as a part of this study) might provide a further insight to the actual failure phenomenon.

Rigid Body Zone

The area of target material contained between the shear front and the slip front has been designated the rigid body zone. In this area, as can be seen in Figure 7, the target material has been displaced almost entirely by a rigid body motion. The material has been moved, i. e., it has been acted upon by real forces; but the observed motion has been as a rigid body. Very little distortion of the painted grids on the target material are observed. The indications are that the forces required to cause the observed movement in this zone would be closely related to depth and surcharge weight.

Symmetry

It was assumed by Terzaghi that the bearing capacity failure plane shape would be two-sided and symmetrical for the theoretical case. In the experimental investigations, few cases of failure plane symmetry were observed, but in almost every test, some asymmetry was observed. At first, it was assumed that this was the result of nonreproducible or improperly aligned loading conditions. Great effort was taken in subsequent tests to eliminate any possible misalignment. This gave little better results. In fact, tests were observed where initial unsymmetrical failure proceeded to a symmetrical failure as penetration continued. No conclusion has been reached as to why the observed asymmetry resulted.

CHAPTER VI

SUMMARY AND CONCLUSIONS

A summary of the experimental investigation conducted and reported in this paper is given in this chapter. The conclusions reached as a result of the study are included. Recommendations for further work that have become apparent from the study performed are also stated.

Summary

An experimental investigation was performed to observe the continuous penetration of a blunt body into a simulated cohesionless soil. The effects of changes of penetrator velocity and width were observed in a series of laboratory tests. A granular cohesionless soil was simulated by using a densely packed array of steel rollers of three different diameters in order to permit visual observation of individual particle movements during failure caused by penetration. The simulated medium selected also permitted the performance of a true two-dimensional study.

The tests were performed in the laboratory using a mechanical actuator and instrumentation that would provide accurate reproducible results. The experimental results have been tabulated and analyzed as reported in Chapter IV.

An examination of present bearing capacity theory was made to determine if the presently postulated mechanism of failure under static loads could be of aid in understanding the mechanism of failure during continuous penetration. The development of the Prandtl-Terzaghi bearing capacity formula was shown and the assumptions made in its derivation were stated.

The failure phenomenon observed in the experimental investigation was described in detail and photographs of pertinent results were included. The failure phenomenon was postulated to contain several finite regions. An edge effects zone was observed to occur adjacent to the penetrator. A wedge zone directly below the penetrator was seen to exist but to be of a transient composition. A distinct shear front proceeded ahead, and to the sides of the penetrator. Far below and well away from the sides of the penetrator, a slip front was observed.

Between the shear front and the edge effects zone, a region of appreciable deformation called the severe shear zone occurred. Movement of the target material accompanied by little deformation was observed in the rigid body zone located between the shear front and the slip front. It was shown that the failure mechanism of continuous penetration was very complex and little understood.

A description of a method of measuring the angle of internal friction of the steel roller target material under a dynamic load was given in Appendix A. The results of measurements made and the value of the angle of internal friction obtained was stated.

Appendix B contains a complete series of sequence photographs taken during one test.

Conclusions

The experimental investigation conducted in this study yields several conclusions. As might be expected, some of these are quite clear, while most are somewhat tentative. This is a result of both the nature of the problem considered and the limited investigation undertaken.

Complex Mechanism

The mechanism involved in the failure of a simulated, granular, cohesionless medium from continuous penetration is very complicated. A comparison of the apparent failure mechanism involved in this case with that postulated for statically loaded footing failure using present theory does not adequately explain the results observed in the experimental investigation.

Penetrator Velocity

The resistance to penetration for a constant width penetrator decreased with increasing velocity of penetration. An understanding of this relationship is not clear at this time. It has been postulated that this behavior may be related in some manner to the inertial effects present during continuous penetration. The above phenomena may be accounted for by the limited velocity ranges investigated. Further studies are needed to establish the factual relationship.

Penetrator Width

An increase in penetrator width resulted in an increase in penetration resistance, but the relationship between resistance increase and penetrator width increase was much less than would be expected. The unit resistance values decreased as the penetrator width increased. No explanation of this behavior has been postulated.

Static Bearing Capacity

The Prandtl-Terzaghi static bearing capacity formula for the general shear case gave results which agreed reasonably with the experimental values for the 1-inch wide penetrator. However, there was no reasonable agreement when wider penetrators were used. The agreement for the smaller penetrator may be pure coincidence. It seems likely, however, that the simple relationships considered by Terzaghi cannot be expected to account for the complicated relationships observed in the continuous penetration process.

Recommendations

This experimental investigation has revealed several areas which require further investigation.

Comparison With Other Theories

Other bearing capacity theories besides the Prandtl-Terzaghi theory should be compared to the results obtained from this experimental investigation. Also, the numerous projectile penetration theories

contained in the literature should be compared to the experimental results obtained.

Further Tests

The test series begun in this investigation should be continued and expanded to include considerably higher velocities and different penetrator widths. The slip front should also be studied in further experiments.

Density Changes

An analysis of the extent and effect of density changes in the severe shear zone that have been observed in these tests should be made. This would appear to be a very fruitful area of study for securing a better understanding of the penetration mechanism.

Shearing Process

An analysis should be made of the effect of the change in angle of shear deformation as the shearing proceeds during penetration that appears to be present in the photographic results of this investigation. If this behavior does occur, that is, if the angle of shear deformation has different values along the shear front or as the shearing action occurs, it would have a profound effect on the development of an understanding of the failure mechanism.

A rigorous analysis of the shearing forces along the observed shear front also should be performed in an attempt to secure some insight into the true relationships that occur during penetration failure.

APPENDIX A

DETERMINATION OF TARGET MATERIAL ANGLE OF INTERNAL FRICTION

It is believed that steel roller bearings have never before been used to simulate soil medium for penetration studies. There were no known published values for the angle of internal friction of such materials. Since the solution of the Prandtl-Terzaghi bearing capacity formula depends upon an accurate knowledge of this value, it became necessary to perform a corollary series of experiments to measure this value. In adapting the Prandtl-Terzaghi formula to a dynamic situation, it was felt that, to be most useful, the value of the angle of internal friction should be obtained under dynamic loading conditions.

Description of Equipment

As part of the general program referred to earlier, a working model was built of a dynamic adaption of the static simple shear apparatus originally conceived by Professor K. A. Roscoe of Cambridge (London) University. This apparatus was used for a series of simple shear tests on the target material at the velocities used in the penetration test series.

A photograph of the dynamic simple shear apparatus set up for this series of tests is shown in Figure 8. The sample holder is 10

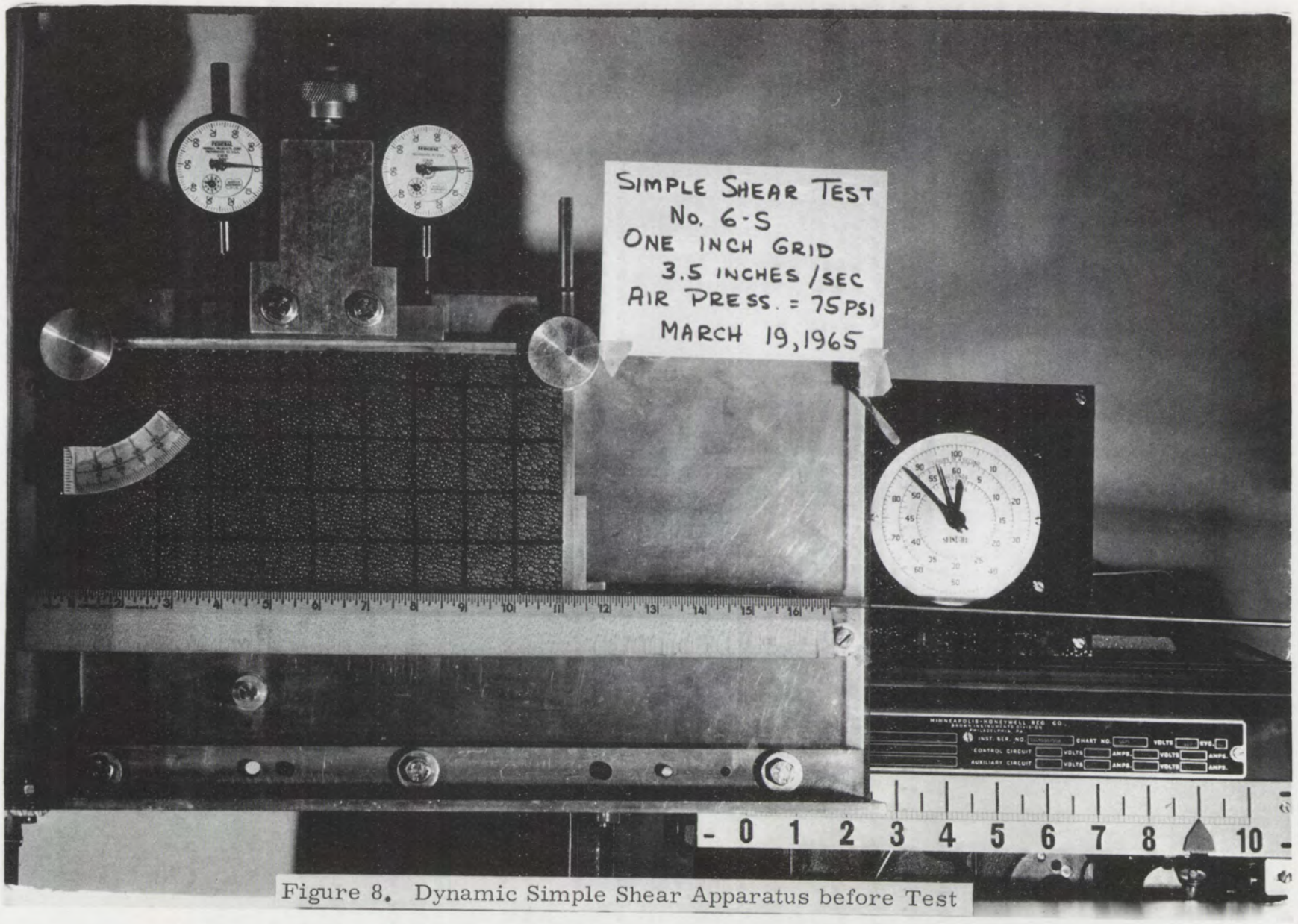

Figure 8. Dynamic Simple Shear Apparatus before Test

inches long, 5 inches high, and 3/4-inch thick, with a face of plexiglas to permit observation of the shearing action. The same linear actuator (not shown in Figure 8) that was used in the penetration test series was arranged to pull the bottom of the sample box to the right. Shown in Figure 8 are the electric clock, two dial indicators to measure sample dialation, the Brown recorder load indicator, and a ruler for measuring displacement. The same sequence camera system used in the penetration series recorded the data from these tests. Although many difficulties and much anguish were experienced in getting this experimental apparatus to perform, the final results were satisfactory and reproducible data were obtained.

Test Procedure

The sample holder of the dynamic simple shear apparatus was filled with steel rollers so that their length coincided with the thickness of the holder. The three different diameters were randomly distributed throughout the array. After the holder was filled, the rollers were adjusted so that the packing (density) equaled that achieved in the large penetration tank (γ = 0.228 pounds/cubic inch). The transparent face was placed on the front of the sample holder and the entire apparatus was reassembled and placed in the test assembly. The linear actuator was connected to the bottom sliding plate of the sample box.

Regulated air pressure was connected to the cylinder fastened to the top plate of the sample holder. By this means, the amount of

surcharge on the top of the sample could be adjusted and controlled during the shearing process.

The test was performed by setting the surcharge air pressure to the desired value. The electric motor driven mechanical actuator was started and the sample holder was pulled through about 40 degrees of rotation at a constant velocity of 2 inches per second. Figure 9 shows the sample holder in the sheared position. This motion caused the target material in the sample holder to be sheared simply. The load required to perform this shearing was measured by the strain gauge and recorded on the Brown recorder as in the regular penetration test series.

Data and Analysis

The data obtained from the dynamic simple shear test of the steel roller bearings are shown in Table IV. The values given are for angle of deformation (shear), ultimate shearing load in pounds, and shearing stress in pounds per square inch. These values are shown for different values of surcharge on the sample surface of 2.1, 5.25, and 7.87 pounds per square inch.

The analysis of the data consisted of plotting the recorded values for angle of shearing deformation versus the shearing stress for the different surcharges used as shown on Figure 10. It was found that, as the simple shear apparatus was deformed to angles greater than 24 degrees, the shearing action tended to deviate from the desired simple

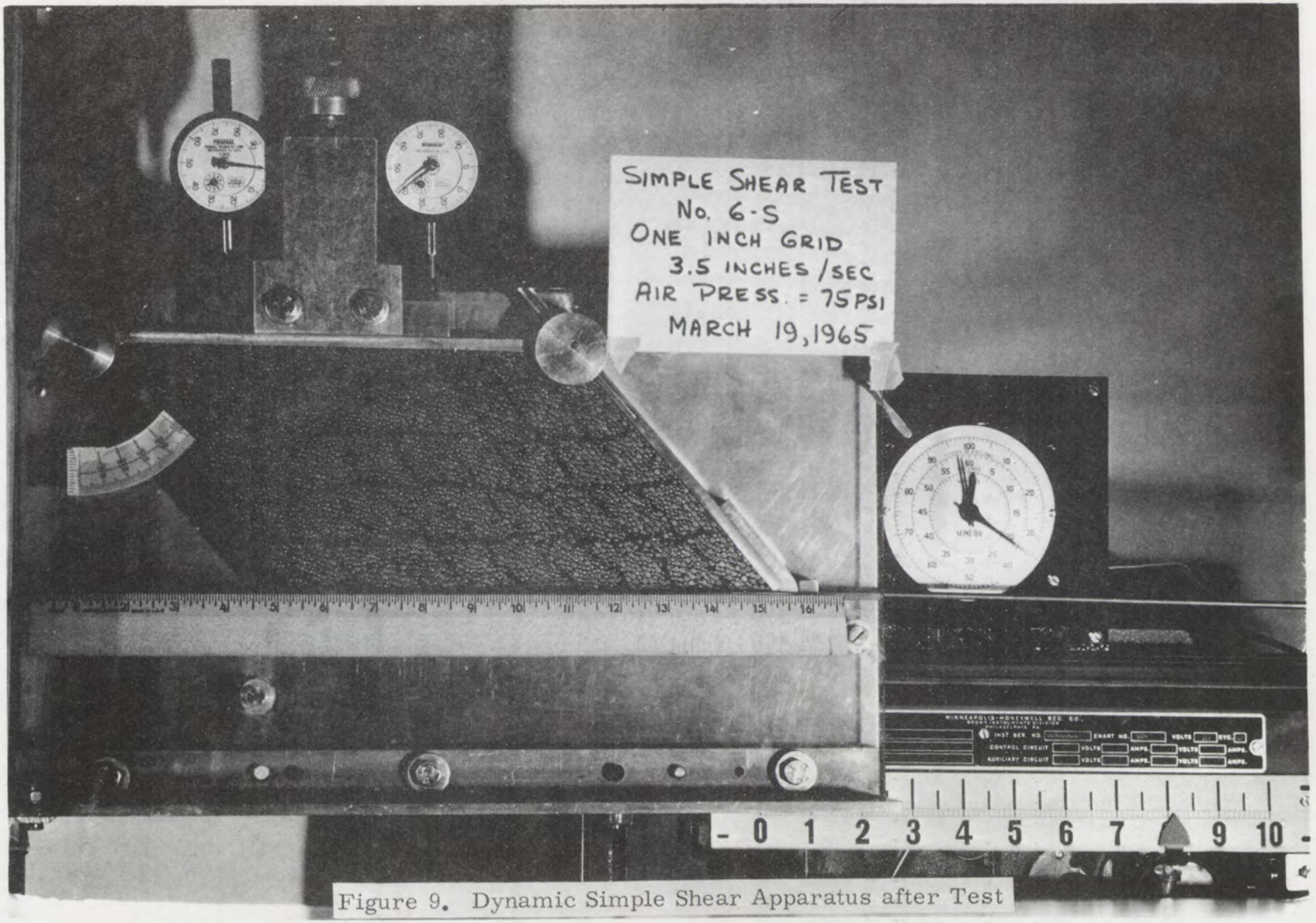

Figure 9. Dynamic Simple Shear Apparatus after Test

Deformation Angle (degrees)	Surcharge = 2.1 psi		Surcharge = 5.25 psi		Surcharge = 7.87 psi	
	Total Load (LB)	Shear Stress (psi)	Total Load (LB)	Shear Stress (psi)	Total Load (LB)	Shear Stress (psi)
0	0	0	0	0	0	0
2.9	13	1.74	24.5	3.28	13	1.74
5.7	14	1.87	26.0	3.47	41	5.46
8.6	15	2.00	26.5	3.54	40	5.34
11.3	16	2.14	26.5	3.54	40	5.34
14.0	16	2.14	27.0	3.61	43	5.74
16.7	16	2.14	31.0	4.14	43	5.74
19.3	16	2.14	40.0	5.34	44	5.88
21.8	18	2.40	46.0	6.14	49	6.54
24.2	25	3.34	58.0	7.75	50	6.67

TABLE IV

Experimental Values from Dynamic Simple Shear Tests

shear mode. The motion of the individual particles of the sample being sheared became erratic, appearing to lock and unlock alternately. Although considerable thought was given to possible causes of this observed phenomenon, no reasonable explanation has been found. Fortunately, observation and measurements of the angles of shear deformation that occur in the vertical penetration tests of the steel roller target medium indicated that deformation angles were quite small. For that reason, simple shear data taken at angles of deformation greater than 24 degrees were arbitrarily deleted.

A Mohr-Coulomb diagram was plotted from the shearing stress data shown in Figure 10 and is shown as Figure 11. The angle of internal friction under dynamic loads for the steel rollers can be obtained directly from this diagram, and the measured values are shown. Because of the small angles of deformation observed in the penetration tests, a value of 30 degrees was chosen for the angle of internal friction to be used in the calculations with the Prandtl-Terzaghi bearing capacity formula.

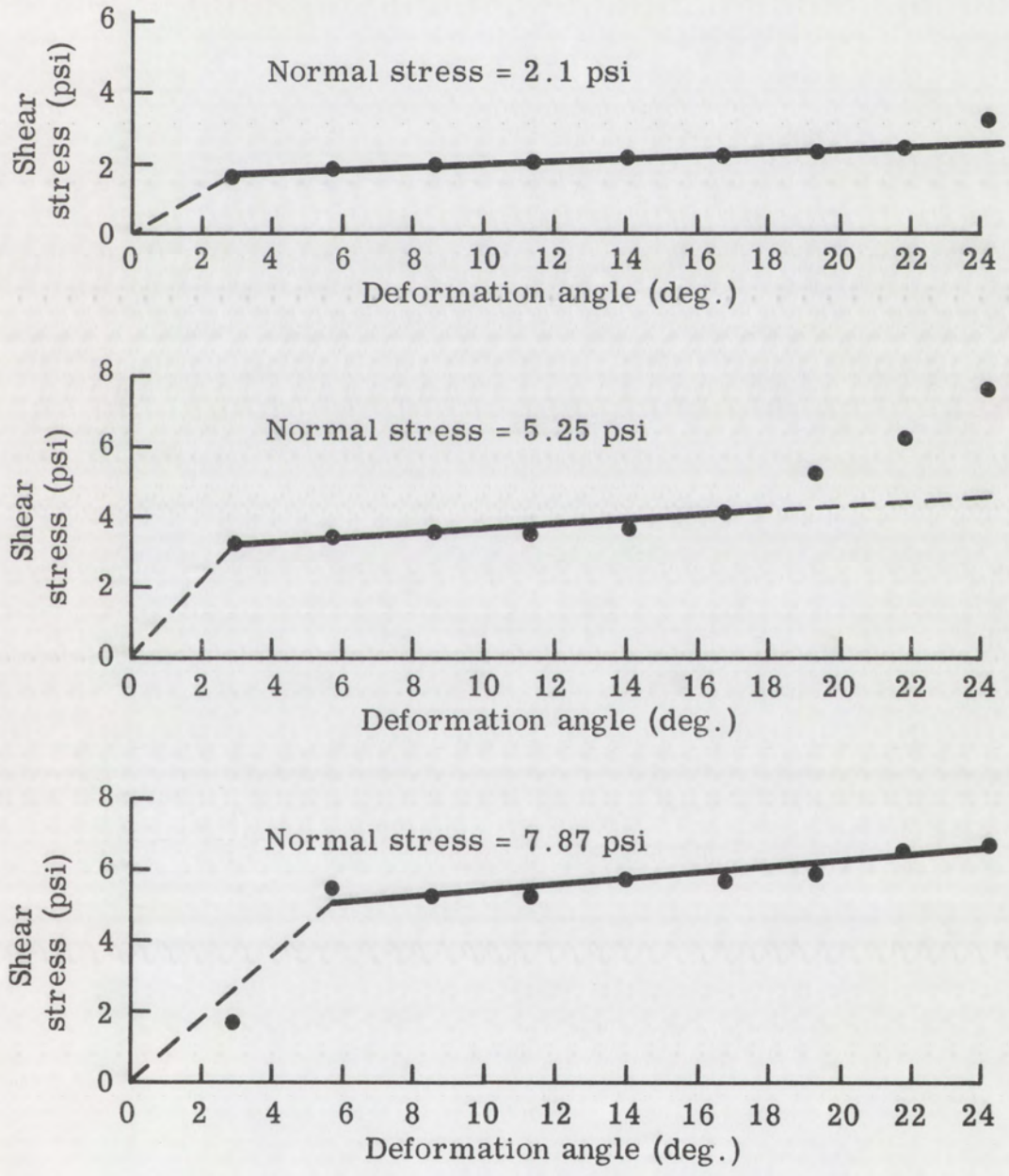

Figure 10. Deformation vs. Shear Stress
Dynamic Simple Shear Data

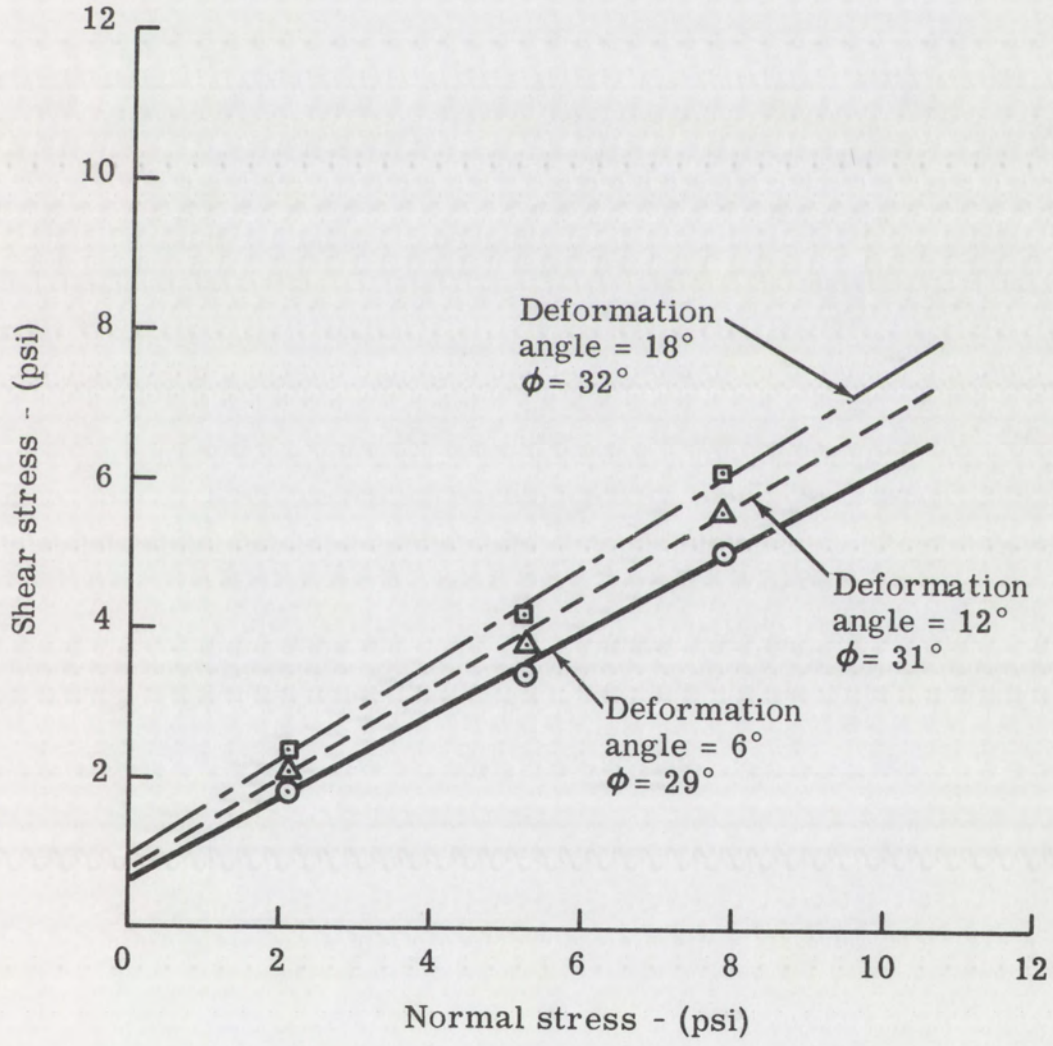

Figure 11. Mohr-Coulomb Diagram
Dynamic Simple Shear Data

APPENDIX B

PHOTOGRAPHIC SEQUENCE OF A PENETRATION TEST

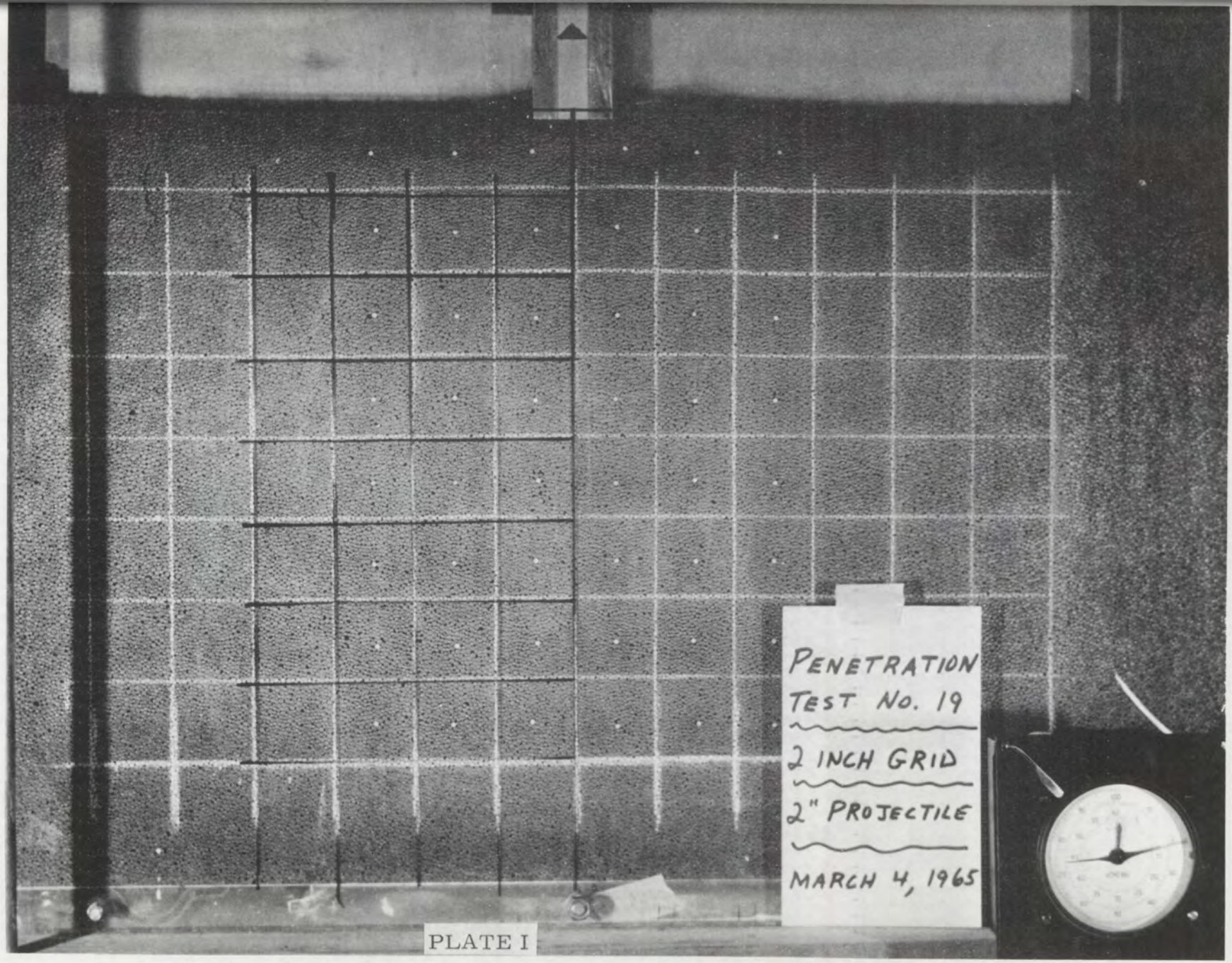

PLATE I

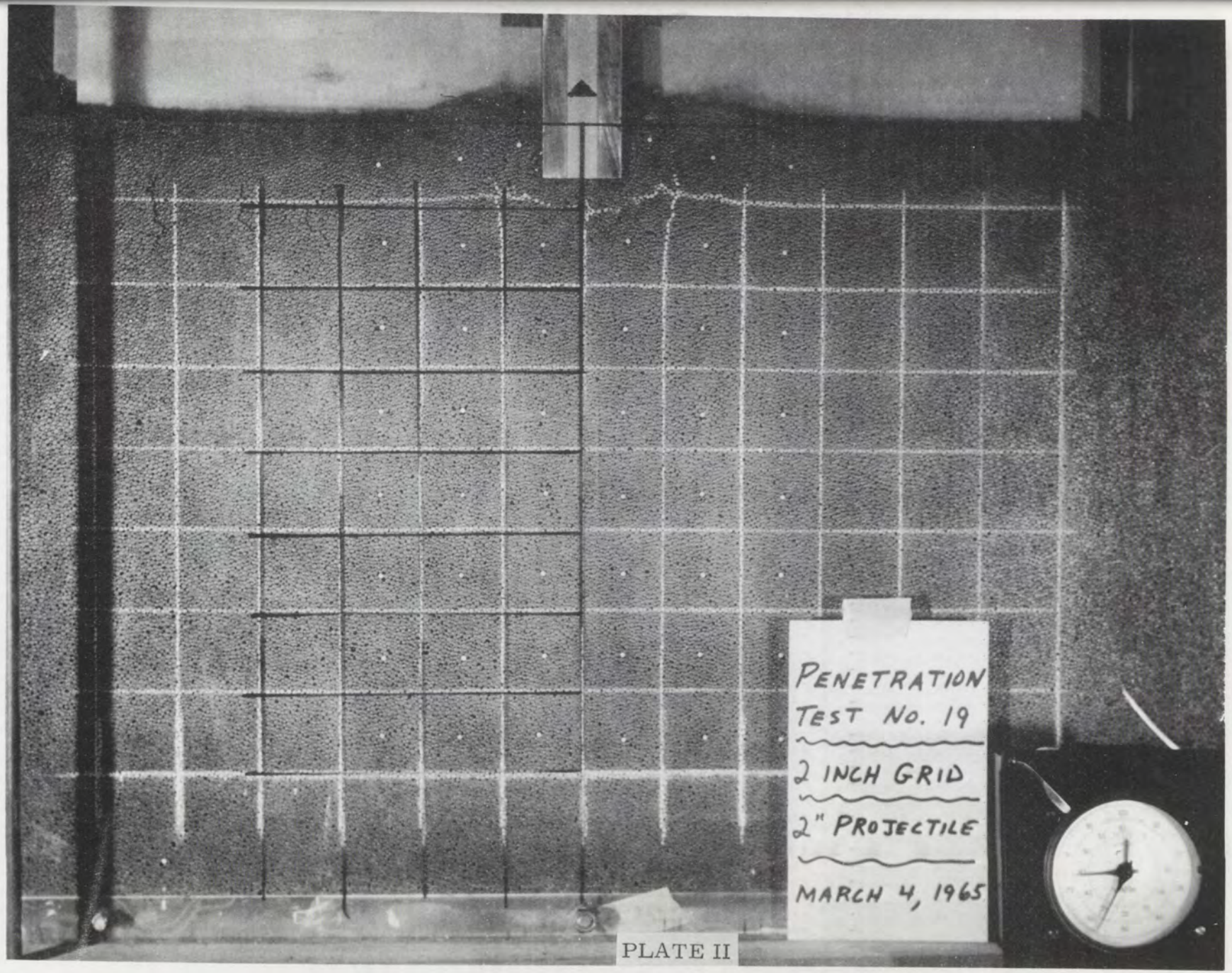

PLATE II

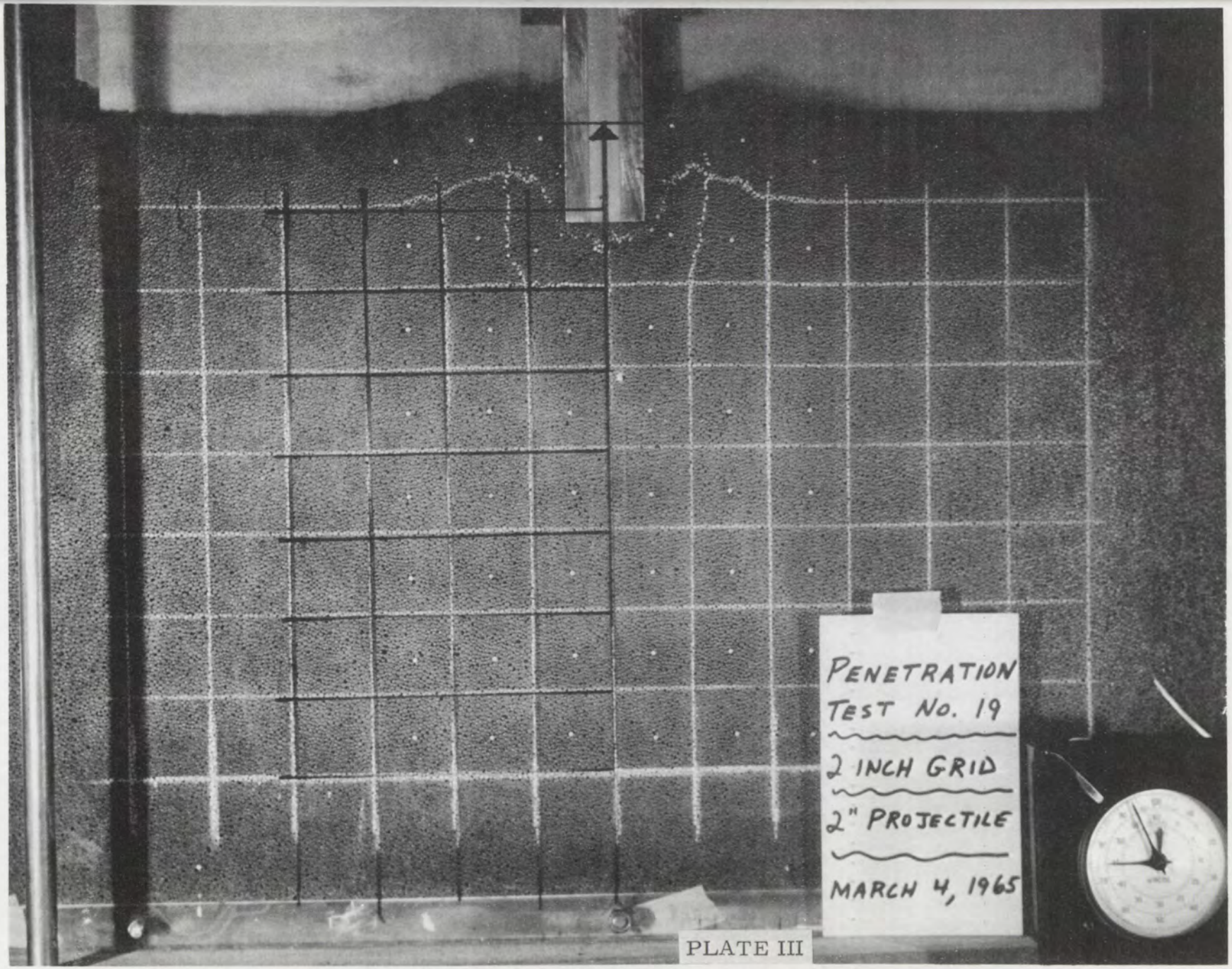

PLATE III

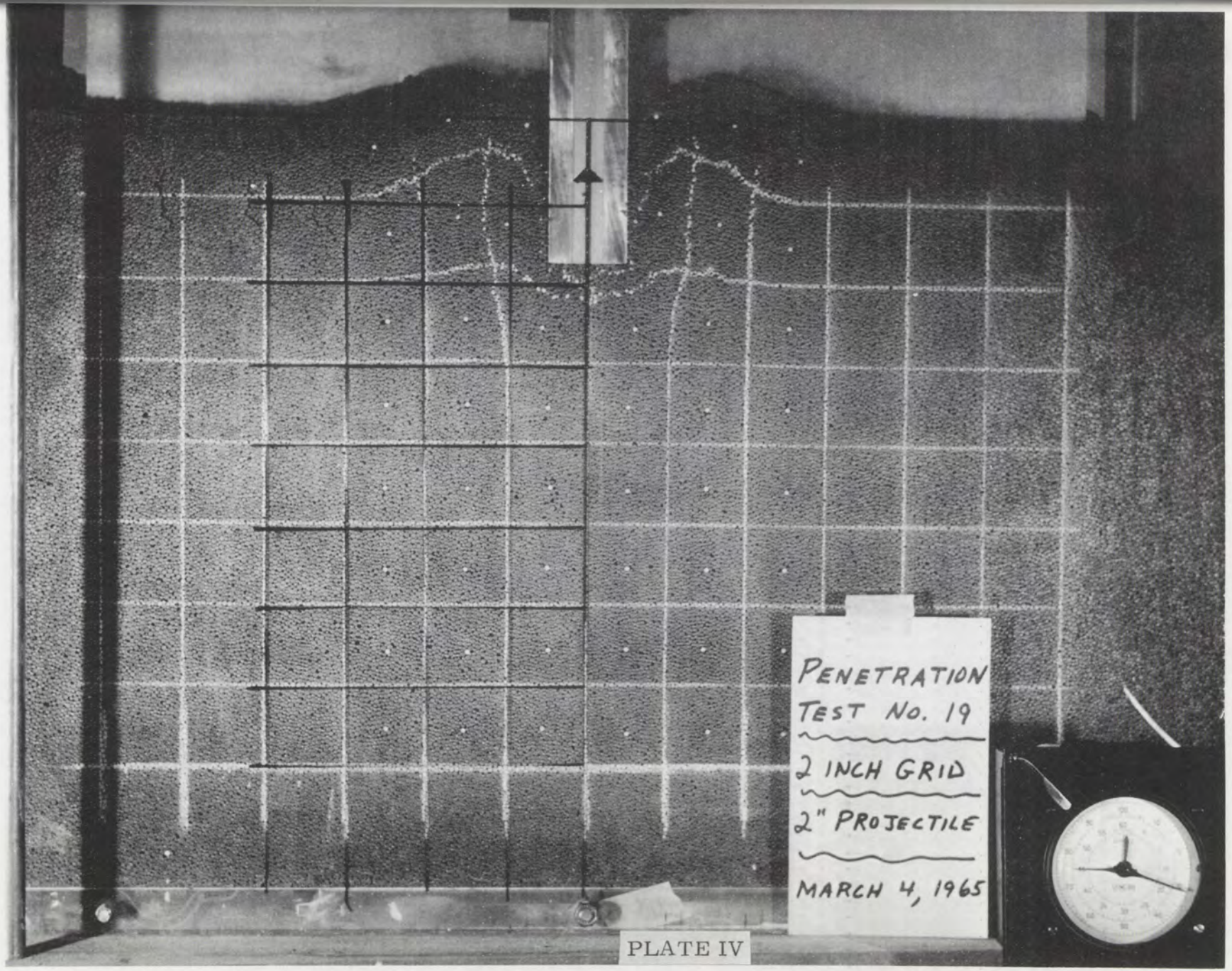

PLATE IV

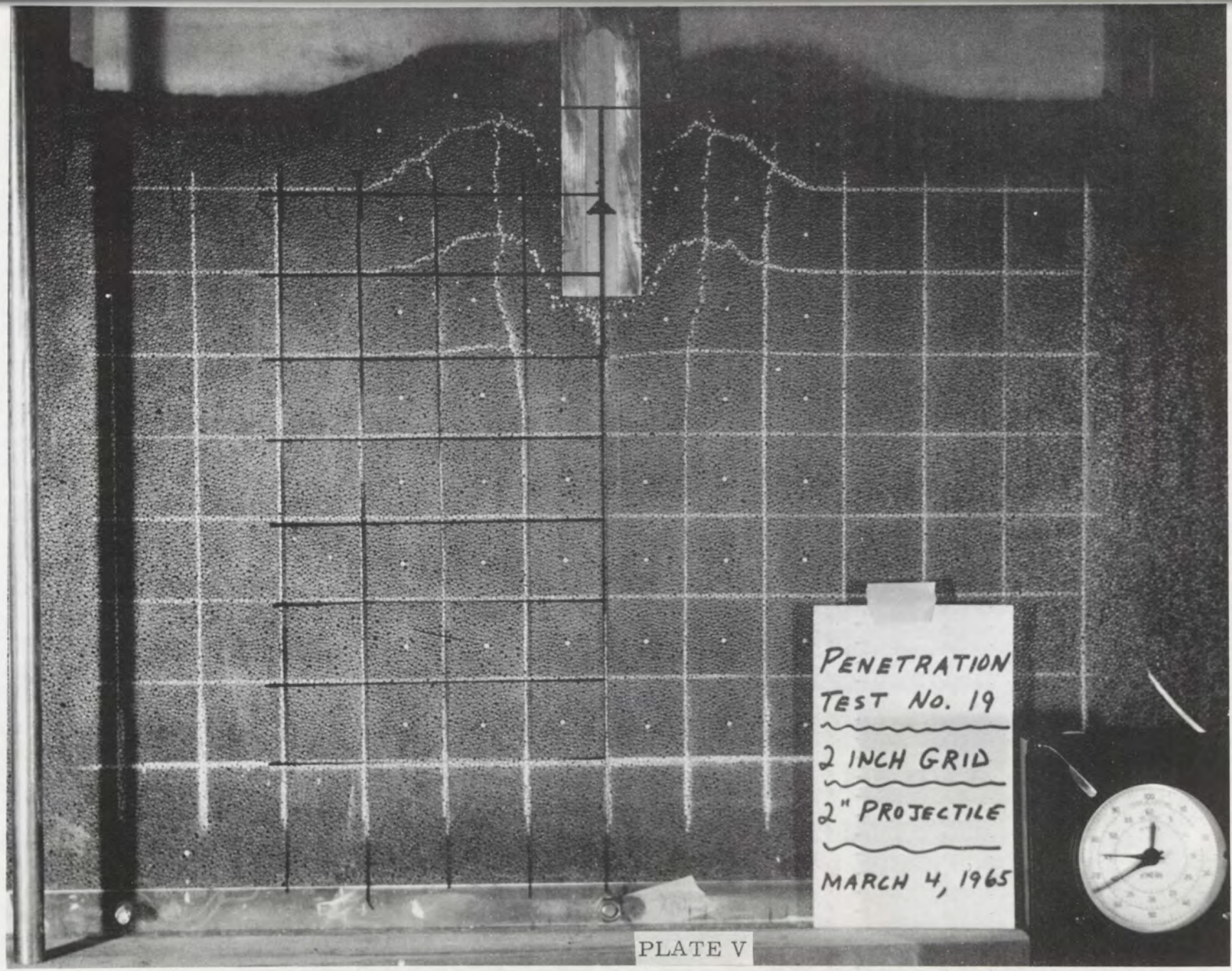

PLATE V

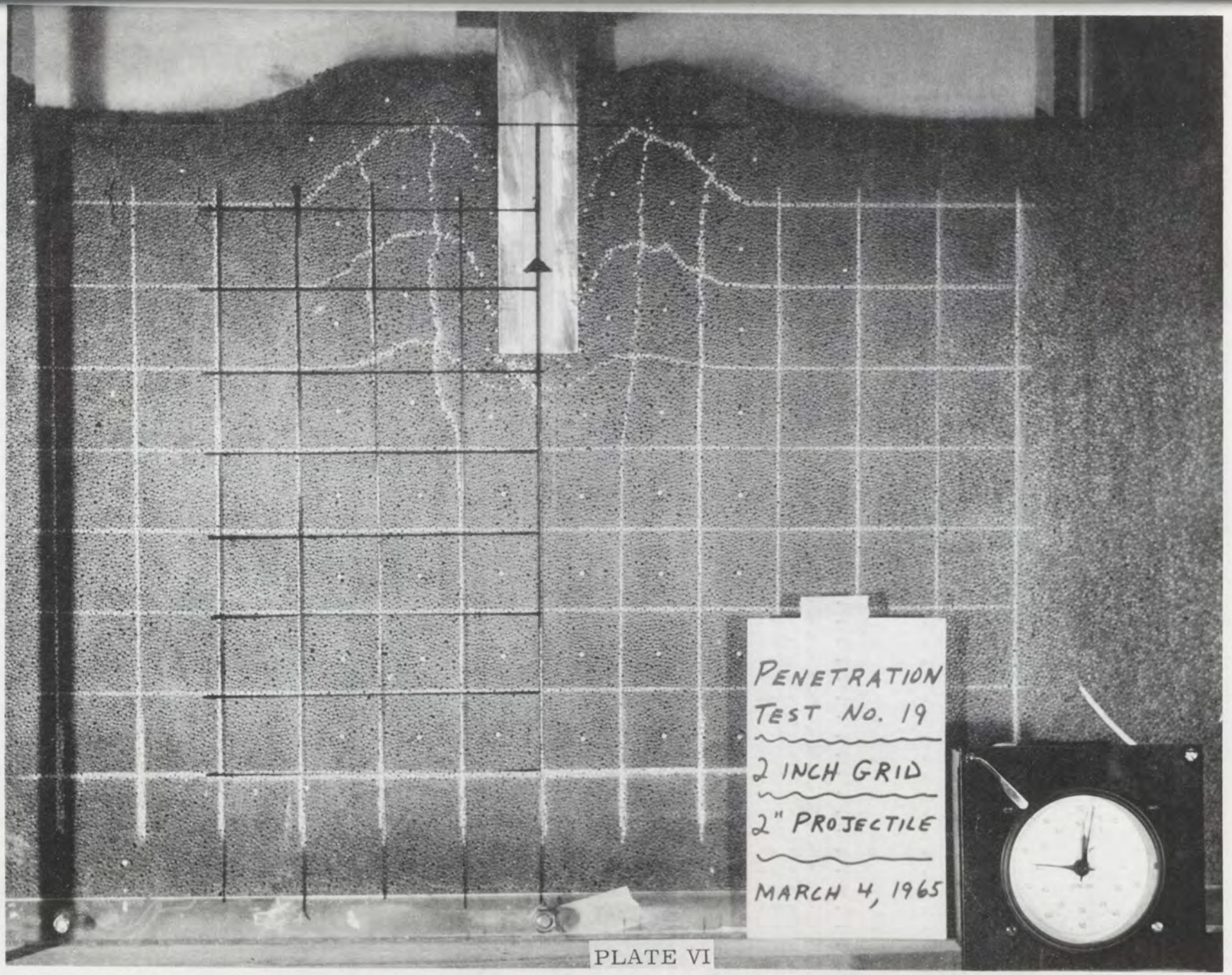

PLATE VI

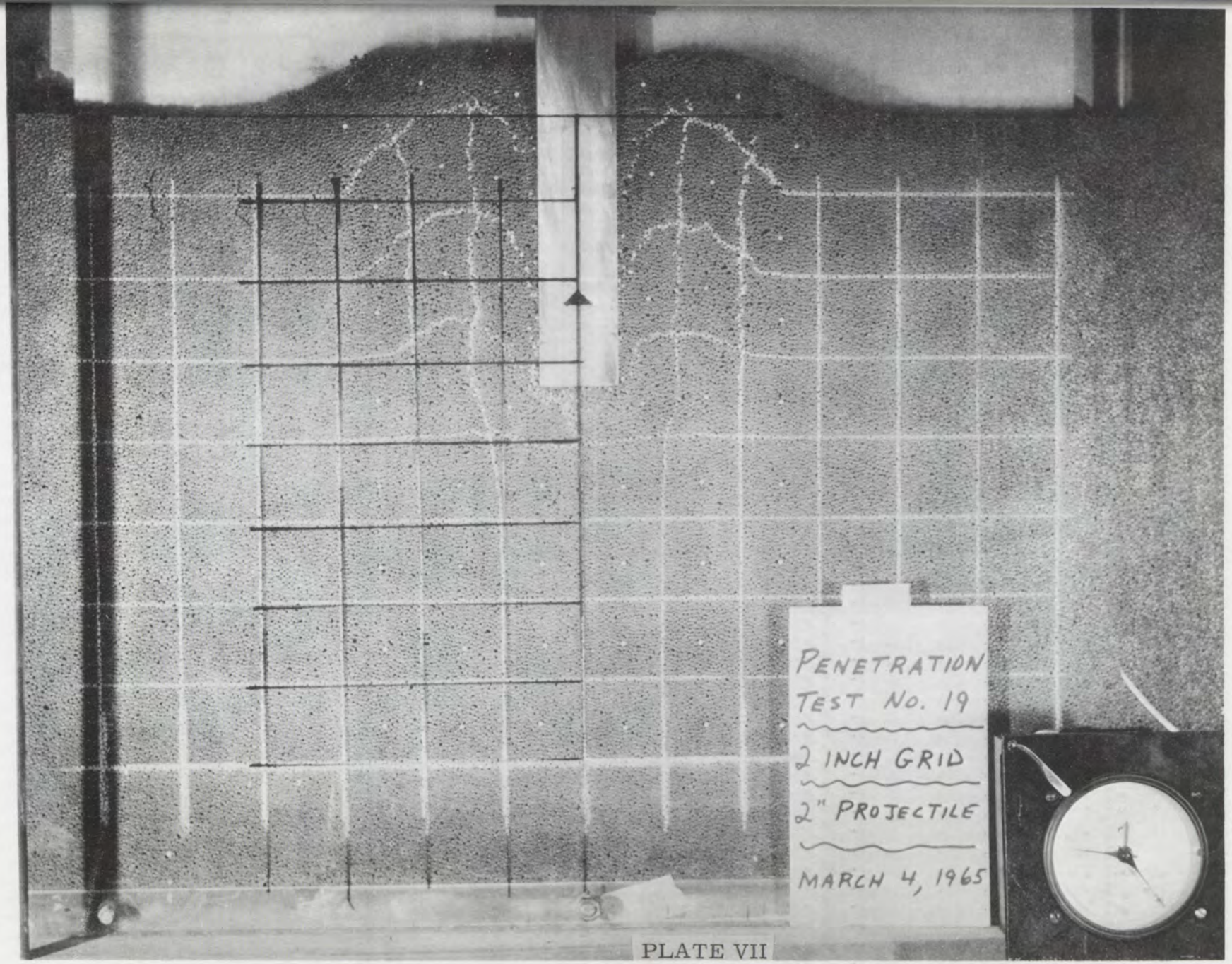

PLATE VII

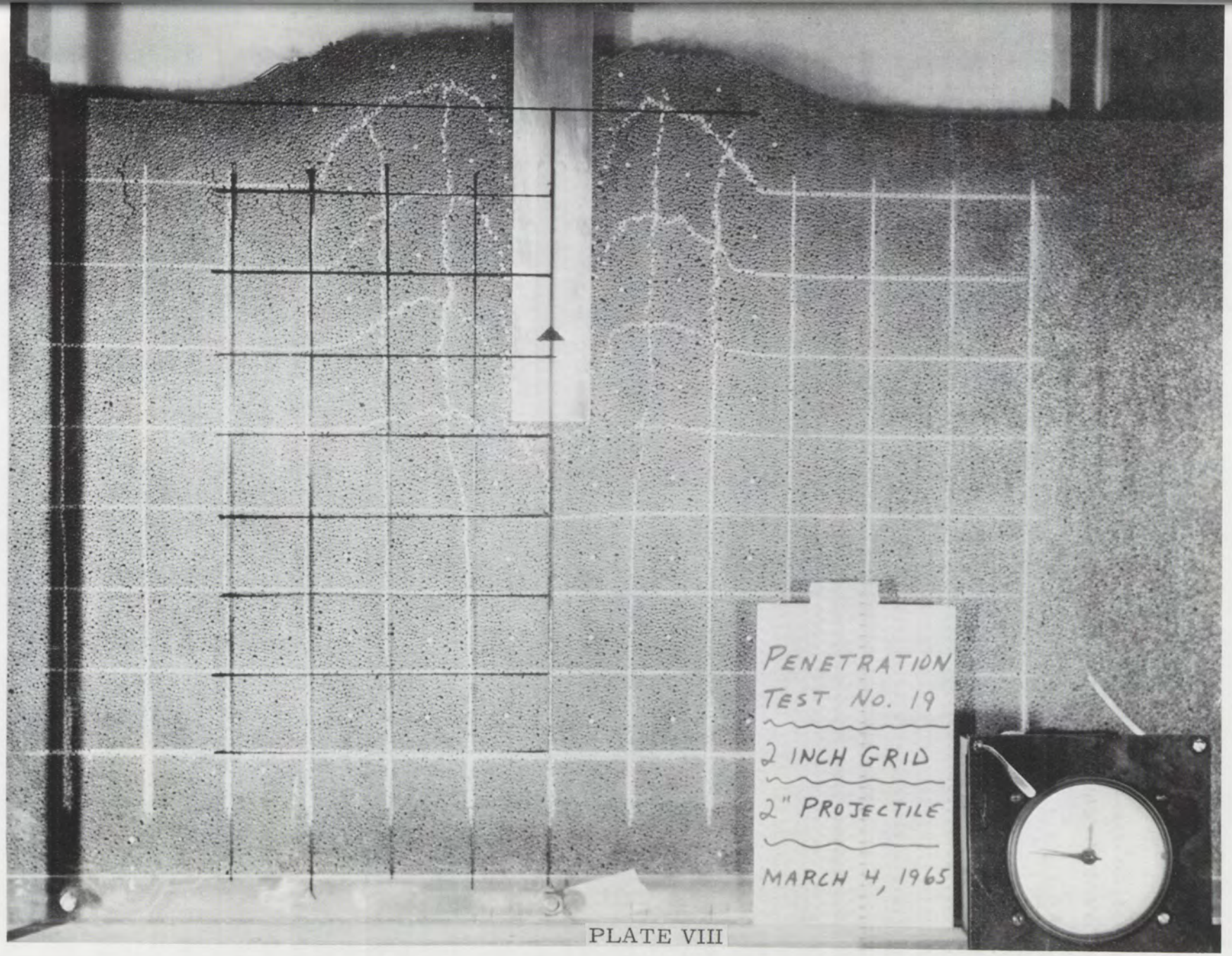

PLATE VIII

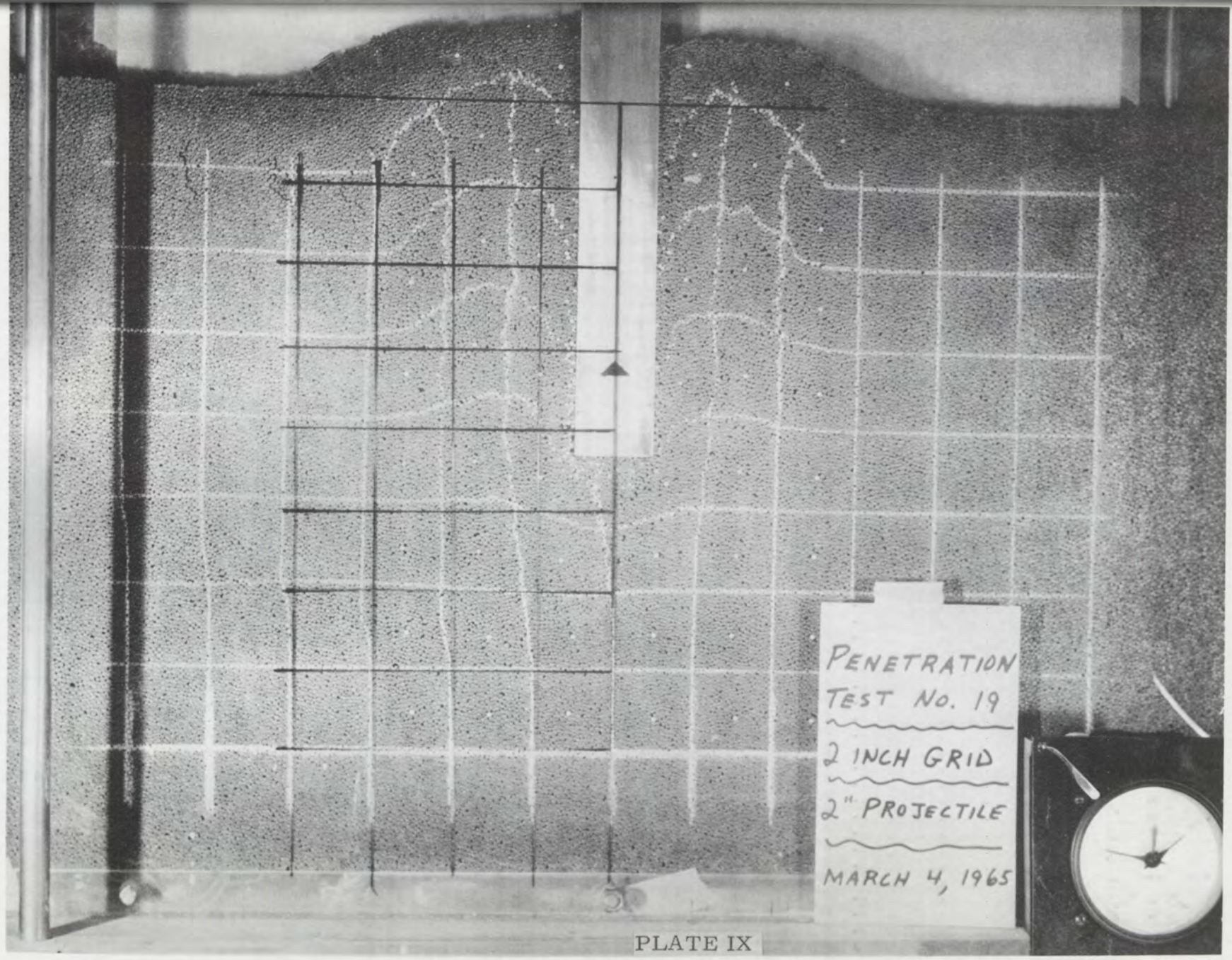

PLATE IX

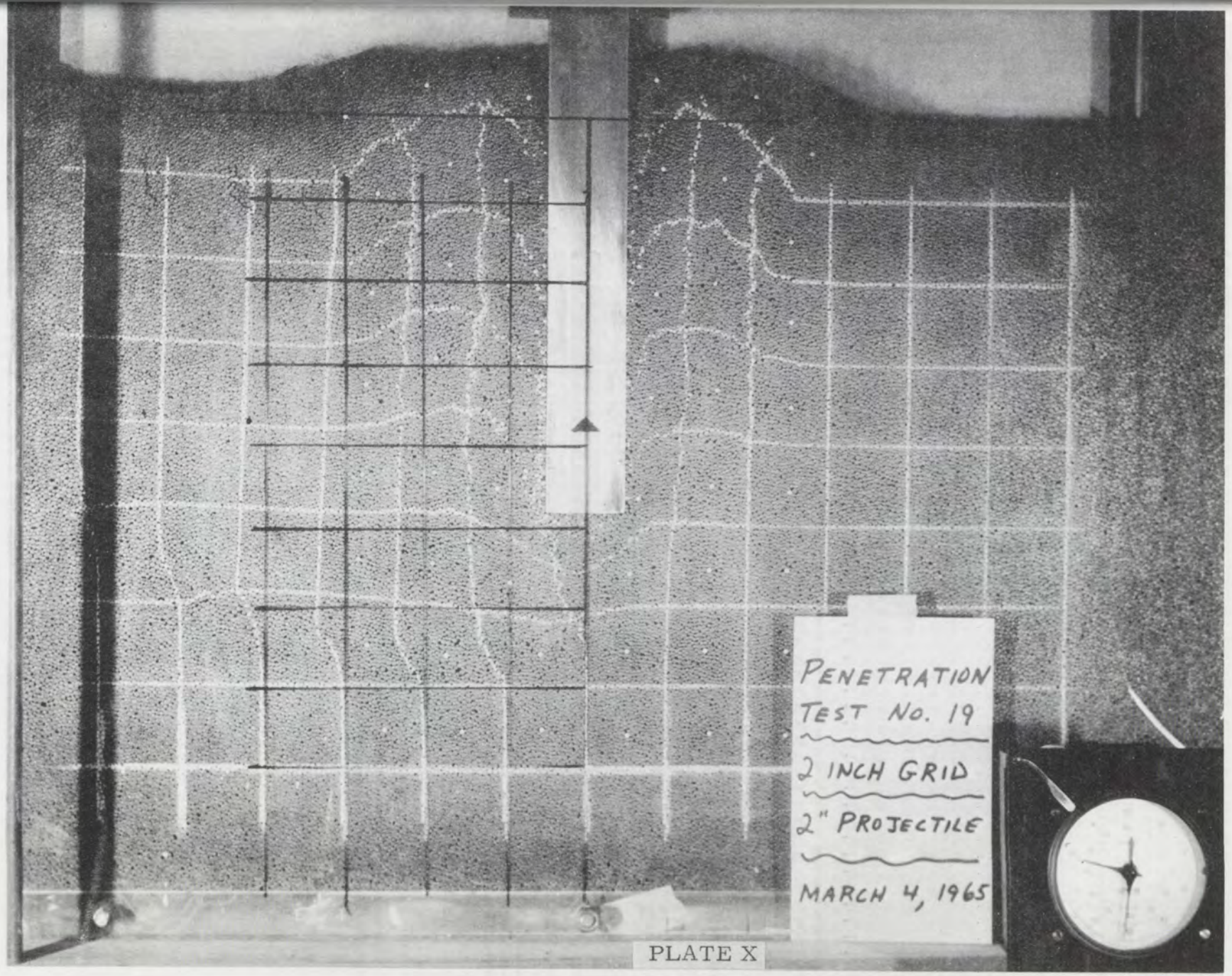

PLATE X

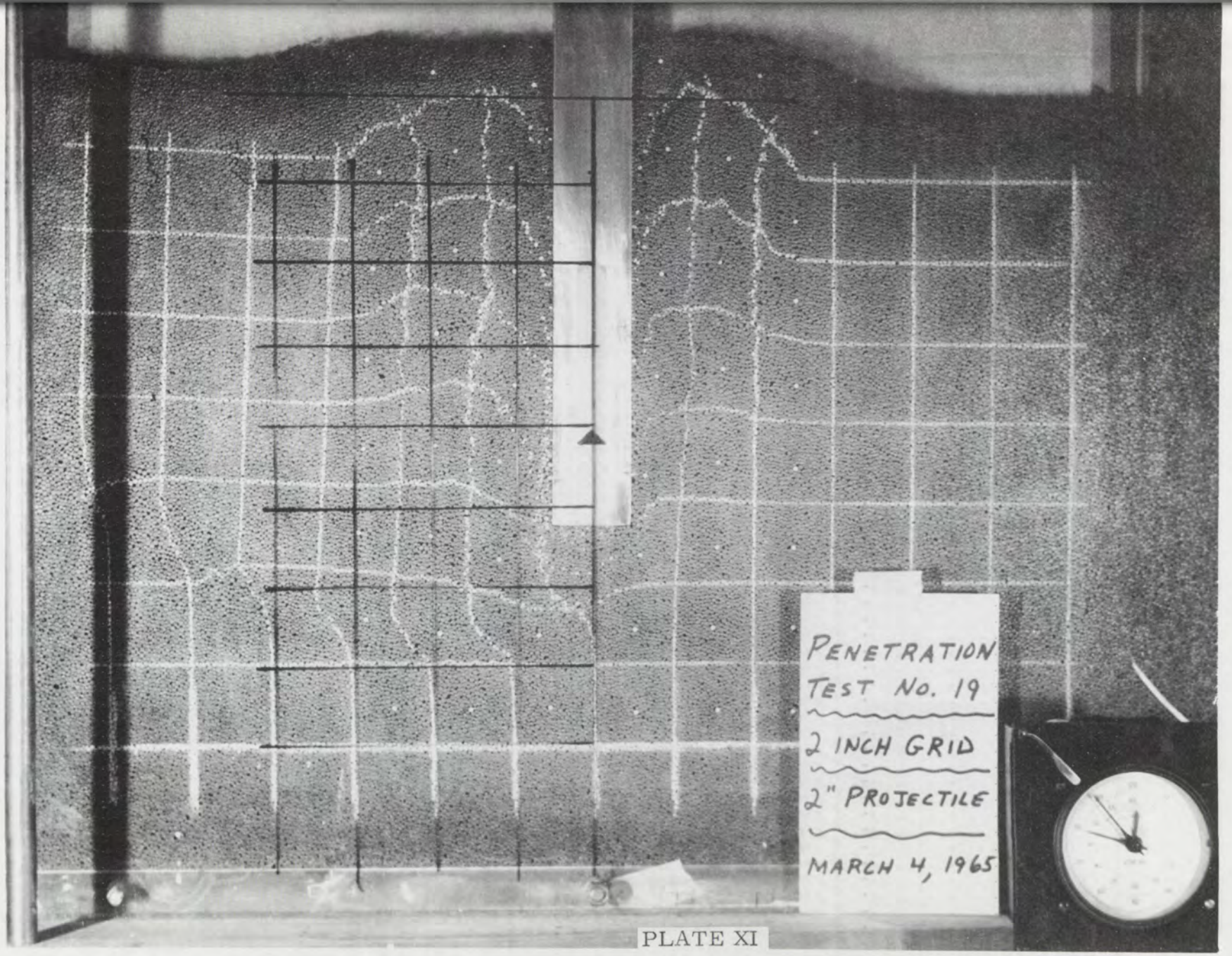

PLATE XI

SELECTED BIBLIOGRAPHY

Braidwood, Robert J. Prehistoric Men. Chicago: Chicago Natural History Museum, 1961, 189 pp.

Hibben, Frank C. The Lost Americans. New York: Thomas Y. Crowell Co., 1946, 200 pp.

Hvorslev, M. Juul. Discussion at Session II - Shallow Foundations, Symposium on Bearing Capacity and Settlement of Foundations, Duke University, April 5-6, 1965.

Jumikis, Alfreds R. Soil Mechanics. Princeton: D. Van Nostrand Company, 1962, 791 pp.

Jumikis, Alfreds R. "Rupture Surfaces in Dry Sand Under Oblique Loads," Journal of Soil Mechanics and Foundation Division, Proceedings, ASCE, Vol. 82, No. SM-1 (January 1956).

Kerisel, Jean. "Deep Foundations Basic Experimental Facts," Paper Presented at Deep Foundations Conference, Mexico D. F., Mexico, December 7-12, 1964.

Leonards, G. A. Foundation Engineering. New York: McGraw-Hill Book Co., Inc., 1962, 1136 pp.

Prandtl, L. Uber Die Harte Plastischer Korper, Nachr. Kgl. Ges. Wiss. Gottingen, Math. Phys. Klasse, 1920.

Robinsky, E. I. and C. F. Morrison. "Sand Displacement and Compaction Around Model Friction Piles," Canadian Geotechnical Journal, Vol. 1, No. 2 (March 1964), pp. 81-93.

Selig, E. T. and K. E. McKee. "Static and Dynamic Behavior of Small Footings," Journal of Soil Mechanics and Foundation Division, Proceedings, ASCE, Vol. 87, No. SM-6 (December 1961), pp. 29-47.

Spangler, M. G. Soil Engineering. Scranton, Pa.: International Textbook Co., 1960, 483 pp.

Terzaghi, Karl. Theoretical Soil Mechanics. New York: John Wiley and Sons, Inc., 1943, 510 pp.

Vesić, A. S., Don C. Banks, and John M. Woodard. "An Experimental Study of Dynamic Bearing Capacity of Footings on Sand," Paper presented at Sixth International Conference on Soil Mechanics and Foundation Engineering, Montreal, Canada, September 1965.